

ROSE

a rotating 4d emittance scanner

M. Maier, L. Groening, C. Xiao, GSI Darmstadt, Germany

A. Bechthold, J. Maus, Neue Technologien GmbH Gelnhausen, Germany

Patent

Phys. Rev. Accel. Beams

ROSE - content

- Slit-grid emittance measurements and the full 4 dimensional beam matrix
- Motivation for measuring, generating or removing interplane beam coupling
- Measurement principle
- Commissioning
- Developing a customer product
 - Hardware - ROSE
 - Electronics* - ROBOMAT
 - Software - ROSOFT
- Summary

* WIPANO

Gefördert durch:



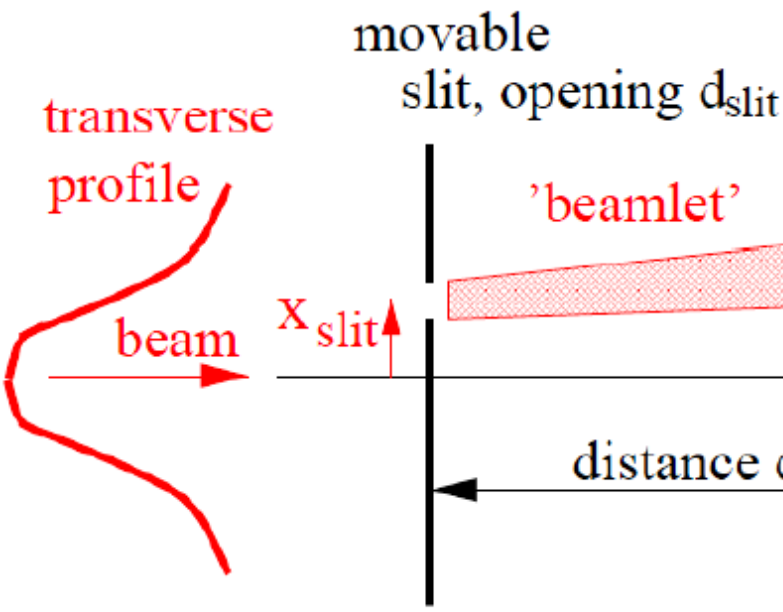
aufgrund eines Beschlusses
des Deutschen Bundestages

ROSE Introduction

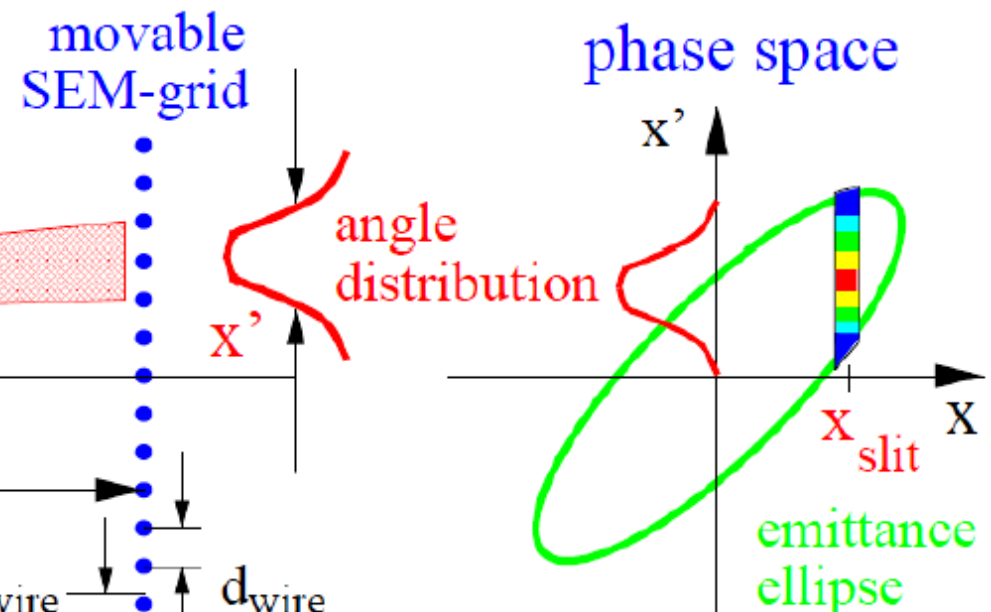
slit grid emittance measurements



Hardware

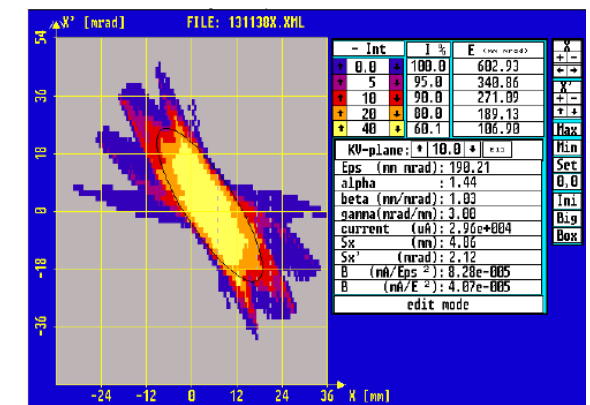


Analysis



*P. Forck, JUAS Archamps

A slit-grid emittance measurement in one plane is integrating over the other plane!

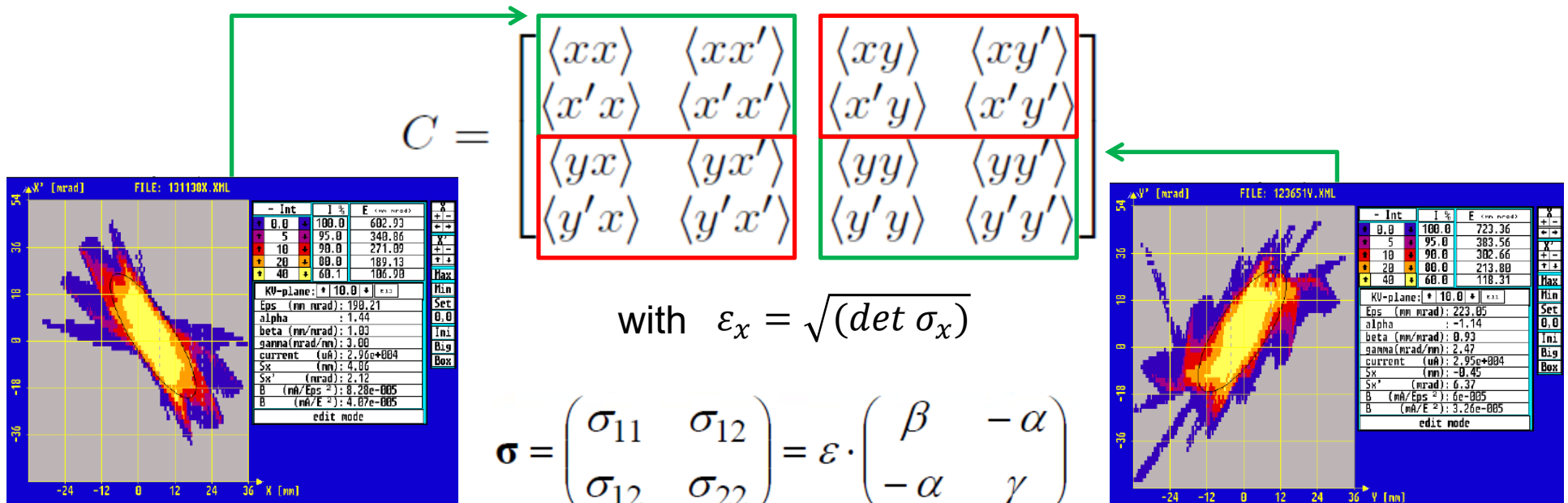


ROSE – introduction

equations for transverse emittance



The four-dimensional symmetric beam matrix C:
For a decoupled beam the off-diagonal matrix elements (red) are zero.



$$\varepsilon_x = \sqrt{\det \sigma} = \sqrt{\sigma_{11}\sigma_{22} - \sigma_{12}^2}$$

α, β, γ are the Twiss parameters and ε_x is the horizontal rms-emittance

ROSE – motivation

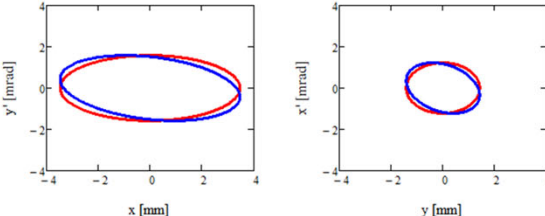
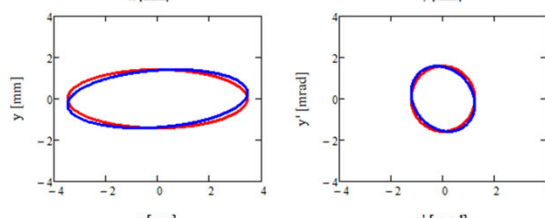
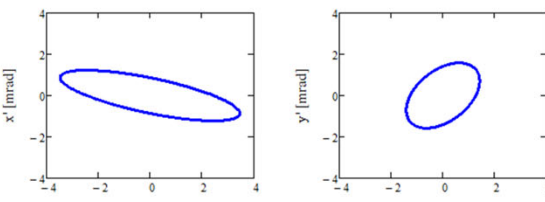
beam envelopes along a solenoid channel



initial beam:

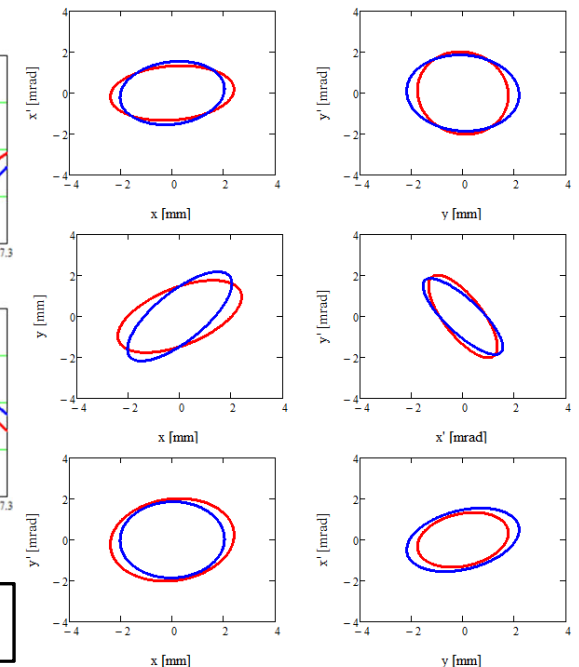
$$C_1 = \begin{bmatrix} 12.00 & -3.00 & 0.00 & 0.00 \\ -3.00 & 1.50 & 0.00 & 0.00 \\ 0.00 & 0.00 & 2.00 & 1.00 \\ 0.00 & 0.00 & 1.00 & 2.50 \end{bmatrix} \text{ uncorrelated}$$

$$C_2 = \begin{bmatrix} 12.00 & -3.00 & 1 & -1.5 \\ -3.00 & 1.50 & -0.5 & -0.35 \\ 1.00 & -0.50 & 2.00 & 1.00 \\ -1.50 & -0.35 & 1.00 & 2.50 \end{bmatrix} \text{ correlated}$$



$$M_{sol} = \begin{bmatrix} C^2 & \frac{SC}{K} & SC & \frac{S^2}{K} \\ -KSC & C^2 & -KS^2 & CS \\ -SC & -\frac{S^2}{K} & C^2 & \frac{SC}{K} \\ KS^2 & -SC & -KSC & C^2 \end{bmatrix}$$

final beam:



red and blue envelopes differ

ROSE – motivation EMTEX

using coupled planes for emittance transfer

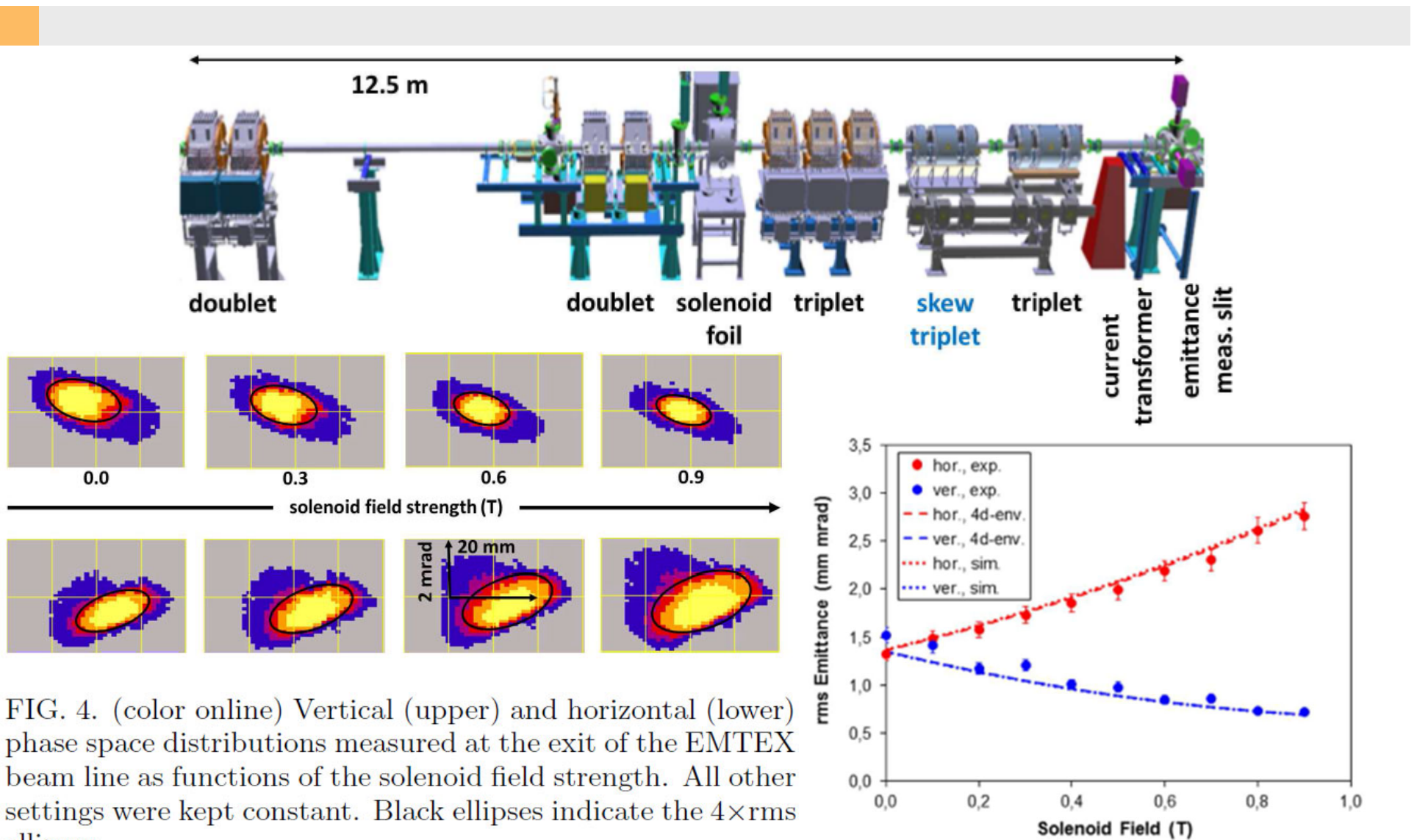
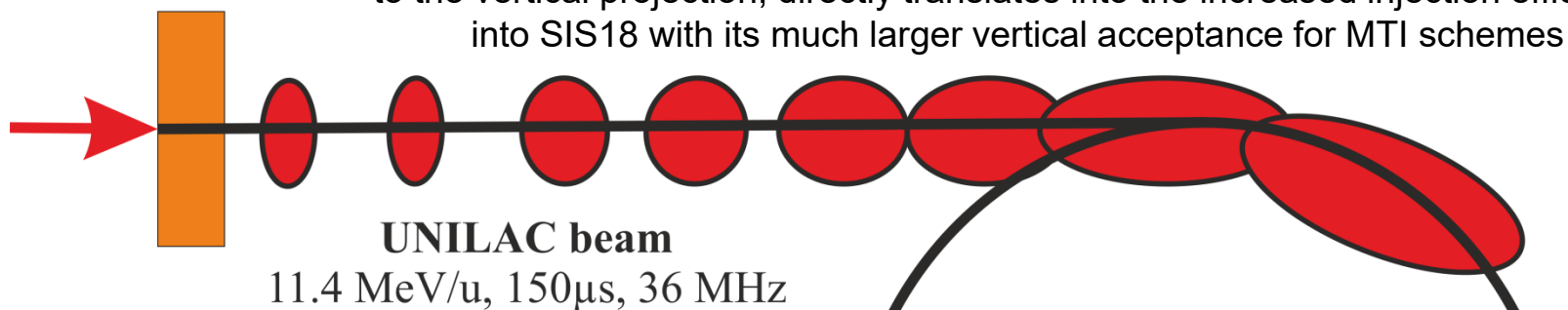


FIG. 4. (color online) Vertical (upper) and horizontal (lower) phase space distributions measured at the exit of the EMTEX beam line as functions of the solenoid field strength. All other settings were kept constant. Black ellipses indicate the $4 \times \text{rms}$ ellipses.

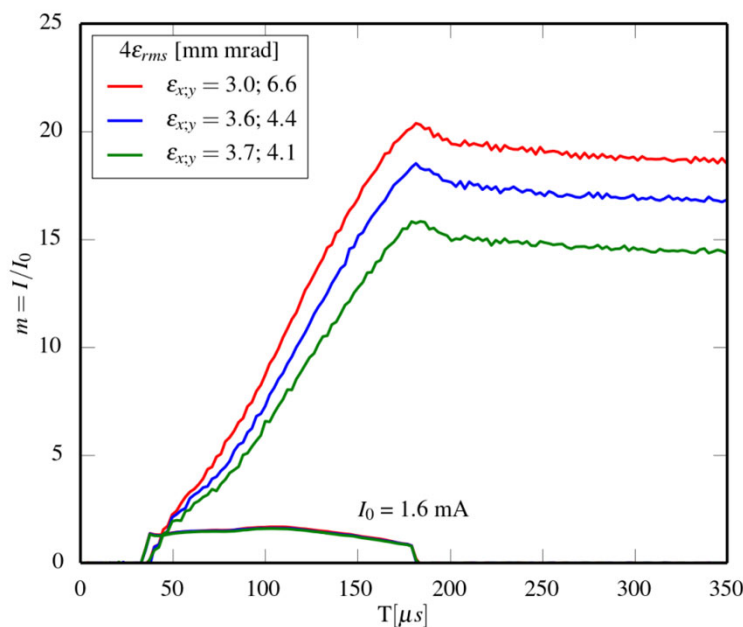
Experimental proof of adjustable single-knob ion beam emittance partitioning, L. Groening, M. Maier, C. Xiao, L. Dahl, P. Gerhard, O.K. Kester, S. Mickat, H. Vormann, and M. Vossberg: *Physical Review Letters*, 113, (2014) 264802

Buncher
BB12



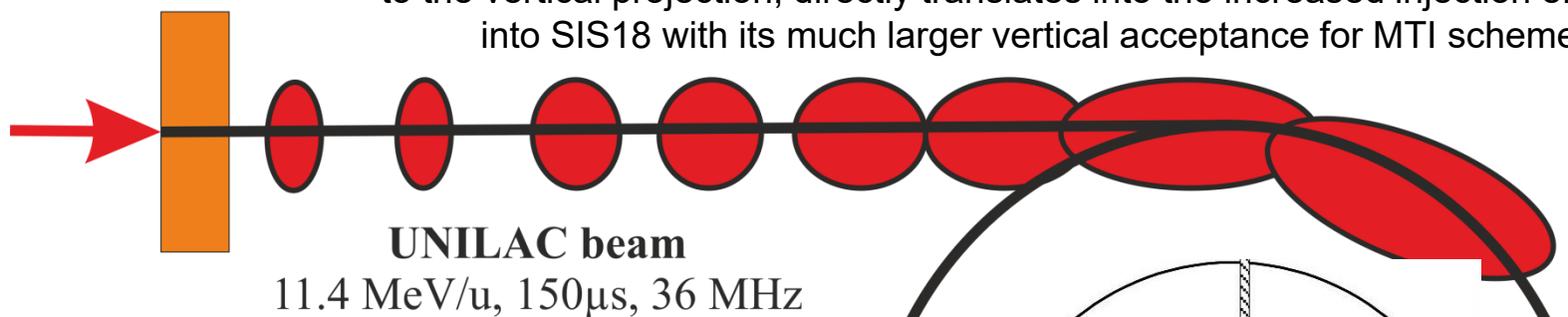
The emittance transfer using EMTEX, shifting beam emittance from the horizontal to the vertical projection, directly translates into the increased injection efficiency into SIS18 with its much larger vertical acceptance for MTI schemes

UNILAC beam
11.4 MeV/u, 150 μ s, 36 MHz

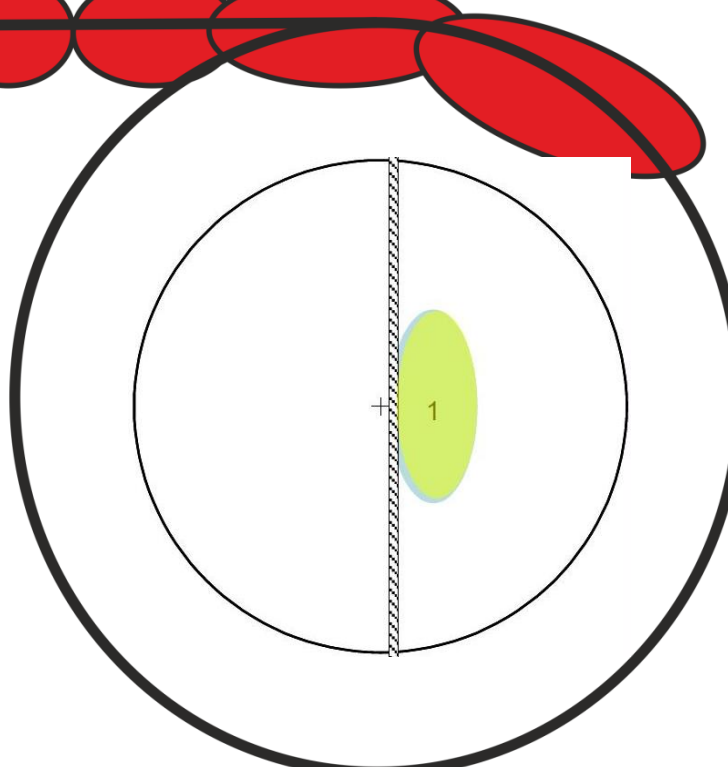
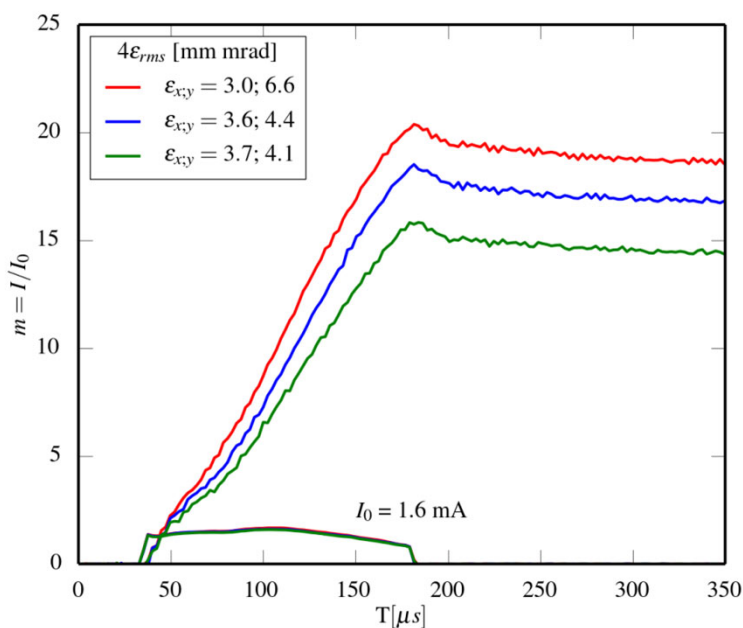


SIS18
 $L = 216 \text{ m}$
 $T = 4.67 \mu\text{s}$
 ~ 20 turn injections

Buncher
BB12

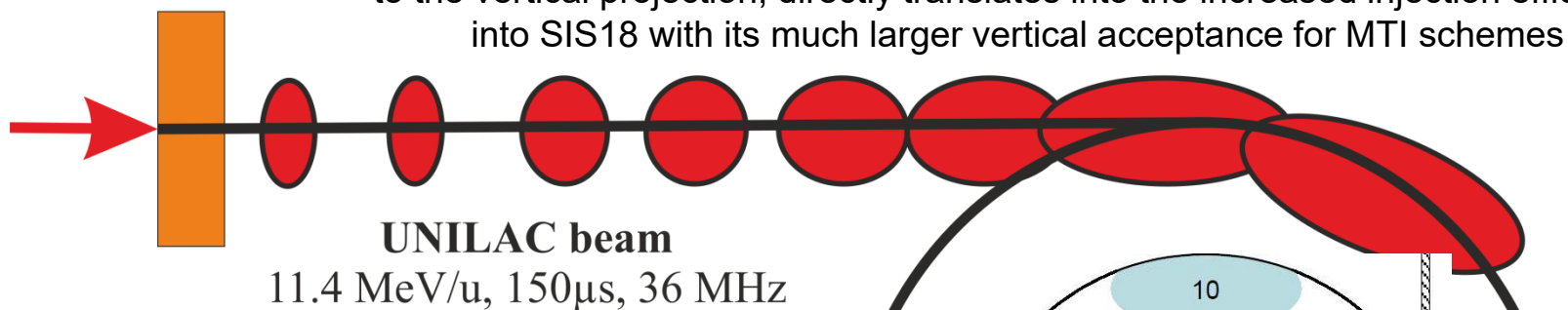


The emittance transfer using EMTEX, shifting beam emittance from the horizontal to the vertical projection, directly translates into the increased injection efficiency into SIS18 with its much larger vertical acceptance for MTI schemes

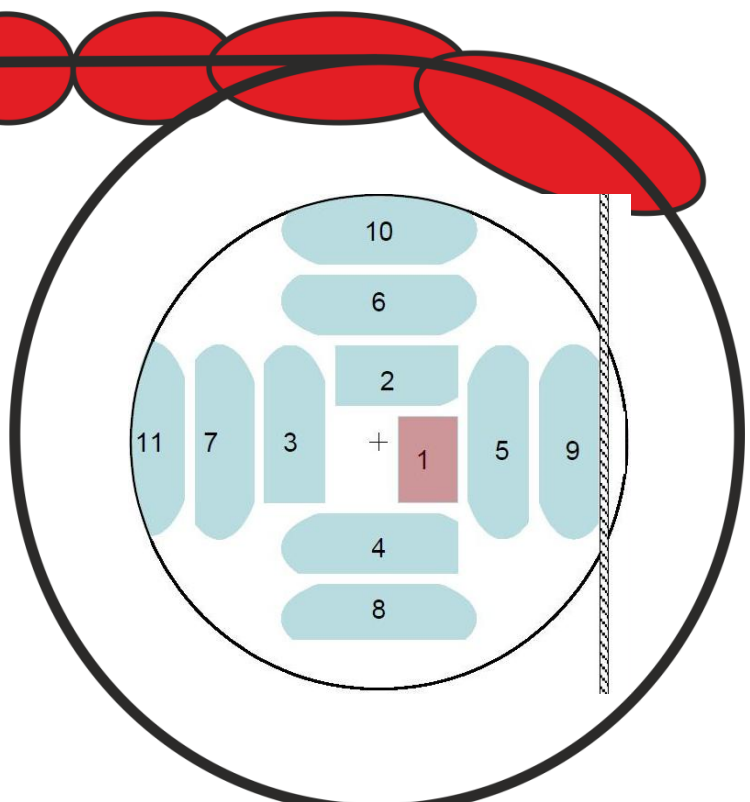
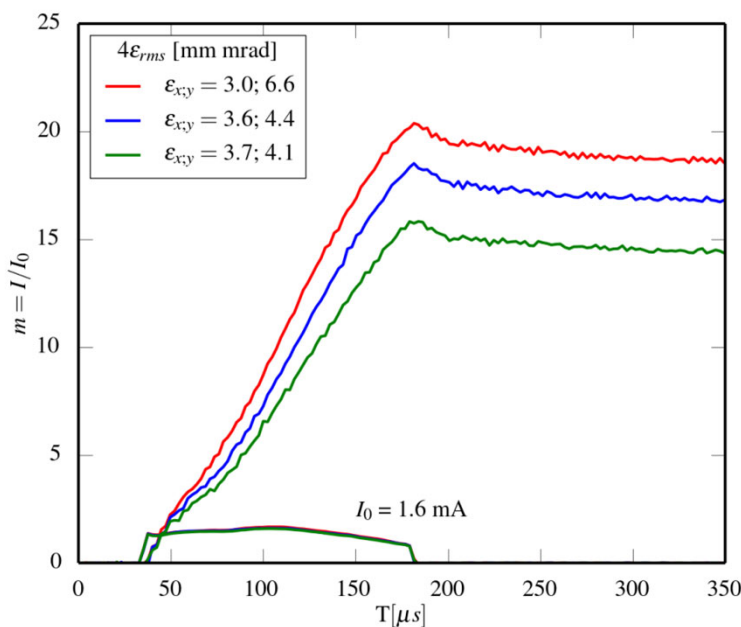


Injection optimization through generation of flat ion beams, S. Appel, L. Groening, Y. El Hayek, M. Maier, C. Xiao: Nucl. Instr. and Meth. A 866, 36-39 (2017), DOI: 10.1016/j.nima.2017.05.041

Buncher
BB12



The emittance transfer using EMTEX, shifting beam emittance from the horizontal to the vertical projection, directly translates into the increased injection efficiency into SIS18 with its much larger vertical acceptance for MTI schemes



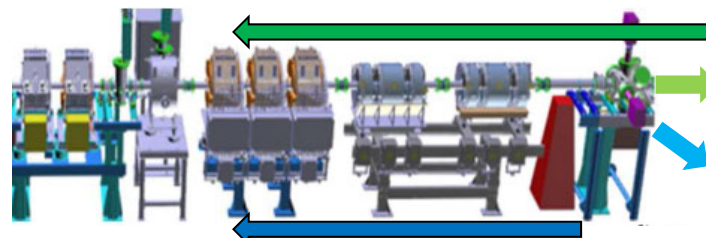
Injection optimization through generation of flat ion beams, S. Appel, L. Groening, Y. El Hayek, M. Maier, C. Xiao: Nucl. Instr. and Meth. A 866, 36-39 (2017), DOI: 10.1016/j.nima.2017.05.041

Rose – motivation coupled Uranium beam for SIS18 injection



Emittance measurements on a 1.7mA $^{238}\text{U}^{28+}$ beam behind the skew quadrupole of EMTEX have been used to measure the 4D emittance. The emittance measurement without using the skew quadrupole assuming an uncorrelated beam at the entrance of EMTEX results in the second-moment beam matrix:

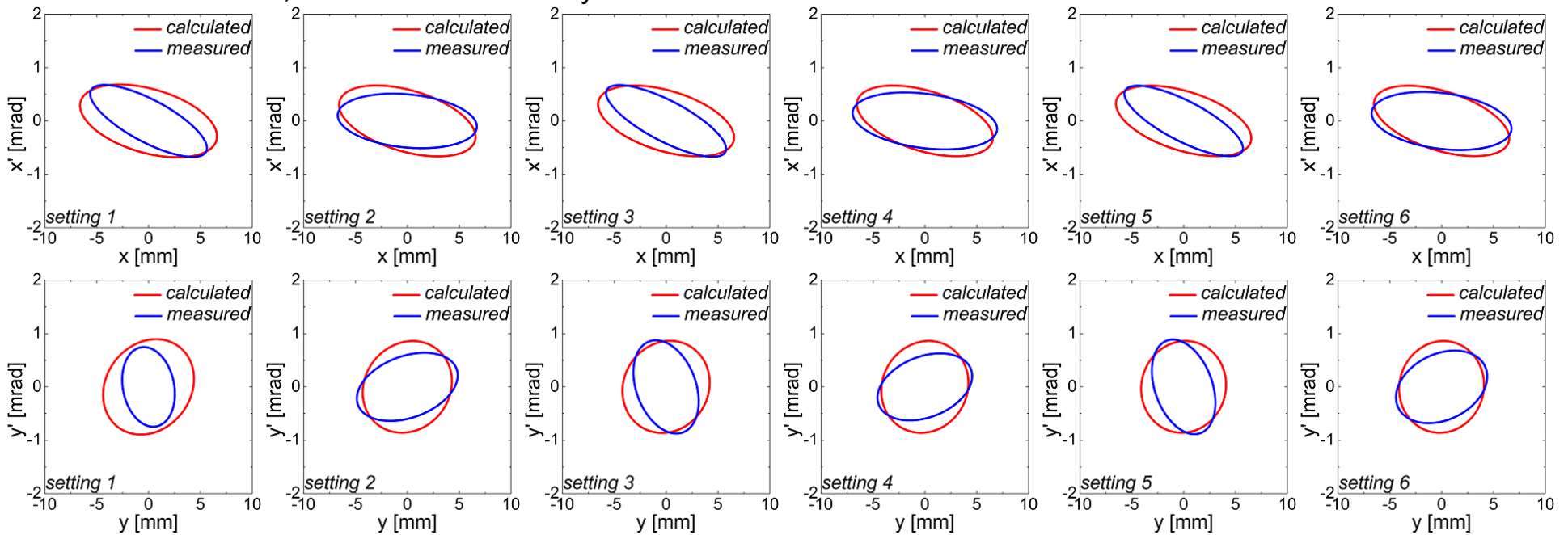
$$C_0 = \begin{pmatrix} 12.79 & 1.89 & 0 & 0 \\ 1.89 & 0.62 & 0 & 0 \\ 0 & 0 & 32.18 & 3.49 \\ 0 & 0 & 3.49 & 0.46 \end{pmatrix}$$



$\alpha_x = -0.902, \alpha_y = -2.160$
 $\beta_x = 6.11, \beta_y = 19.89 \text{ m/rad}$
 $\varepsilon_x = 2.1, \varepsilon_y = 1.6 \text{ mm*mrad}$

setting 1–6

Repeating the measurements for turned on skews and comparing them to the simulations, using the above uncorrelated matrix, does not fit sufficiently well! Thus it is concluded the initial beam inhabits correlations.

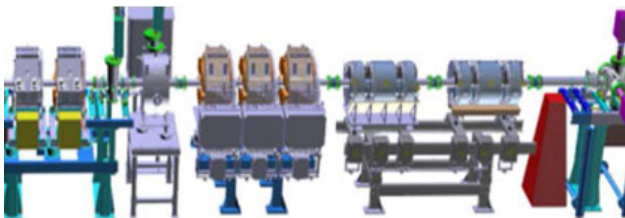


Rose – motivation coupled Uranium beam for SIS18 injection



A method has been developed to determine the coupling moments. The resulting second-moment beam matrix at the entrance is:

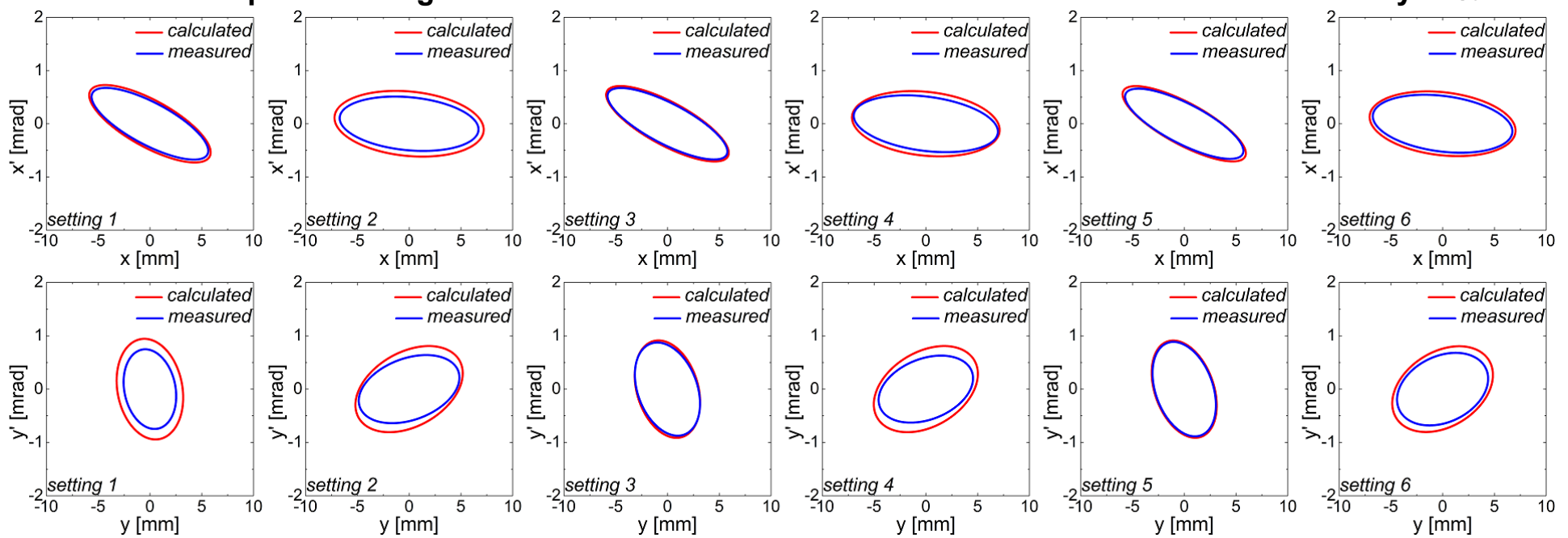
$$C'_{\text{0}} = \begin{pmatrix} 12.79 & 1.89 & 0.18 & 0.37 \\ 1.89 & 0.62 & 1.69 & 0.29 \\ 0.18 & 1.69 & 32.18 & 3.49 \\ 0.37 & 0.29 & 3.49 & 0.46 \end{pmatrix}$$



$$\varepsilon_1 = 2.1, \varepsilon_2 = 1.2 \text{ mm*mrad}$$

coupling parameter t = 0.342

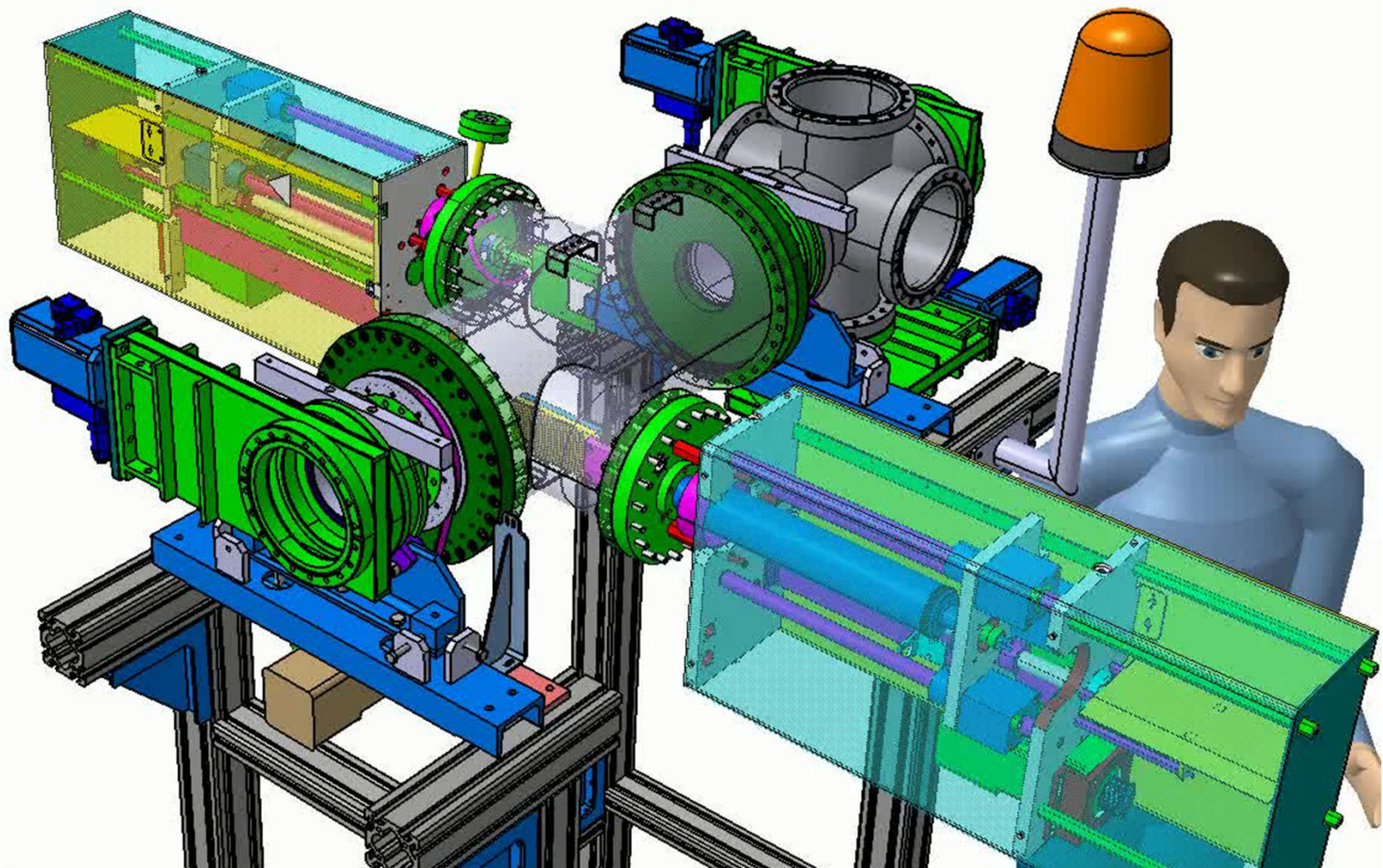
**To our knowledge this is the first successful measurement of the 4D-rms-emittance of ions ≥ 150 keV/u.
In this example removing the correlation would allow for an increase of the beam brilliance by 75%.**



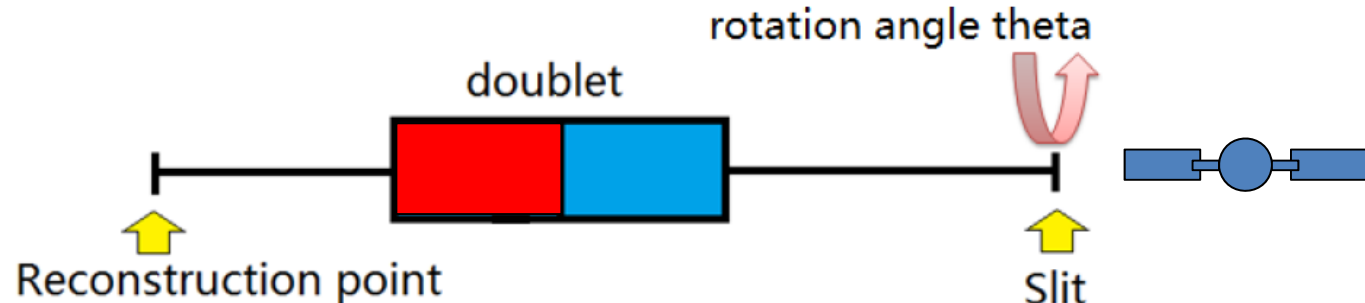
Measurement of the transverse four-dimensional beam rms-emittance of an intense uranium beam at 11.4 MeV/u, C. Xiao, L. Groening, P. Gerhard, M. Maier, S. Mickat, H. Vormann: NIMA 2016, doi: 10.1016/j.nima.2016.02.090

ROSE – technical description

instead of rotating the beam we could:



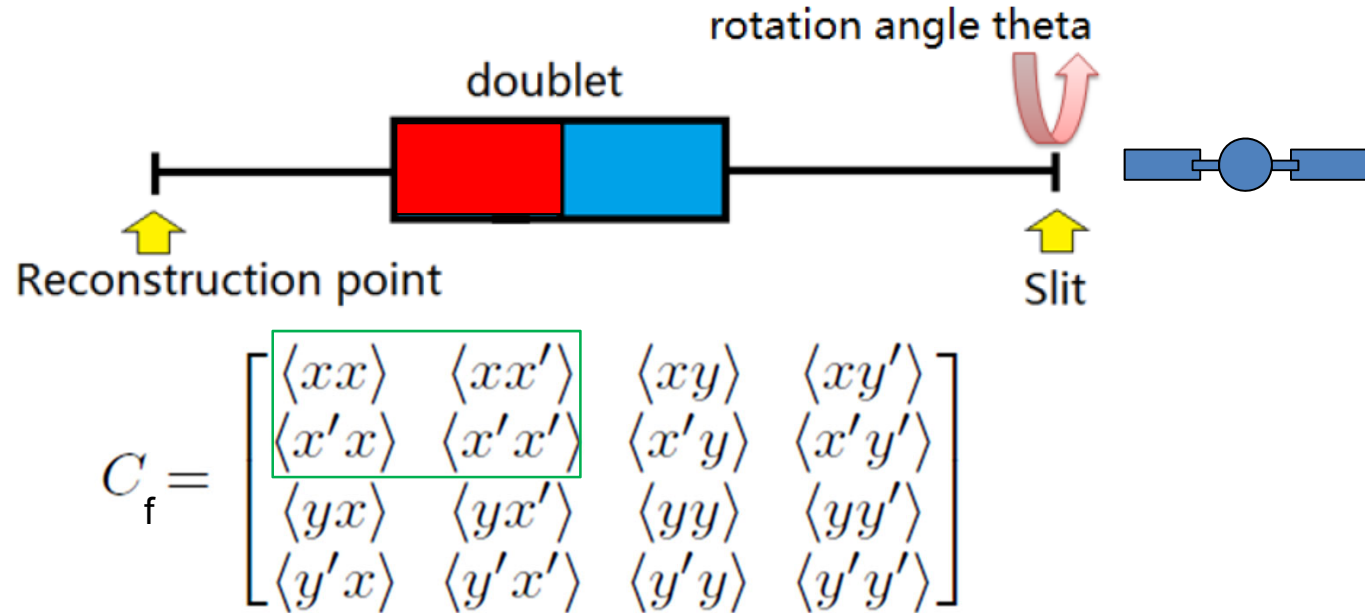
ROSE – measurement principle



$$C_f = \begin{bmatrix} \langle xx \rangle & \langle xx' \rangle & \langle xy \rangle & \langle xy' \rangle \\ \langle x'x \rangle & \langle x'x' \rangle & \langle x'y \rangle & \langle x'y' \rangle \\ \langle yx \rangle & \langle yx' \rangle & \langle yy \rangle & \langle yy' \rangle \\ \langle y'x \rangle & \langle y'x' \rangle & \langle y'y \rangle & \langle y'y' \rangle \end{bmatrix}$$

All values are measured using Rose behind a magnetic doublet at the final position C_{final} . Knowing the transfer matrix they can be calculated back to the reconstruction point of the original not changing beam matrix C_{initial} . 100% transmission between initial and final Position and full slit-grid coverage is of course required for all magnet settings.

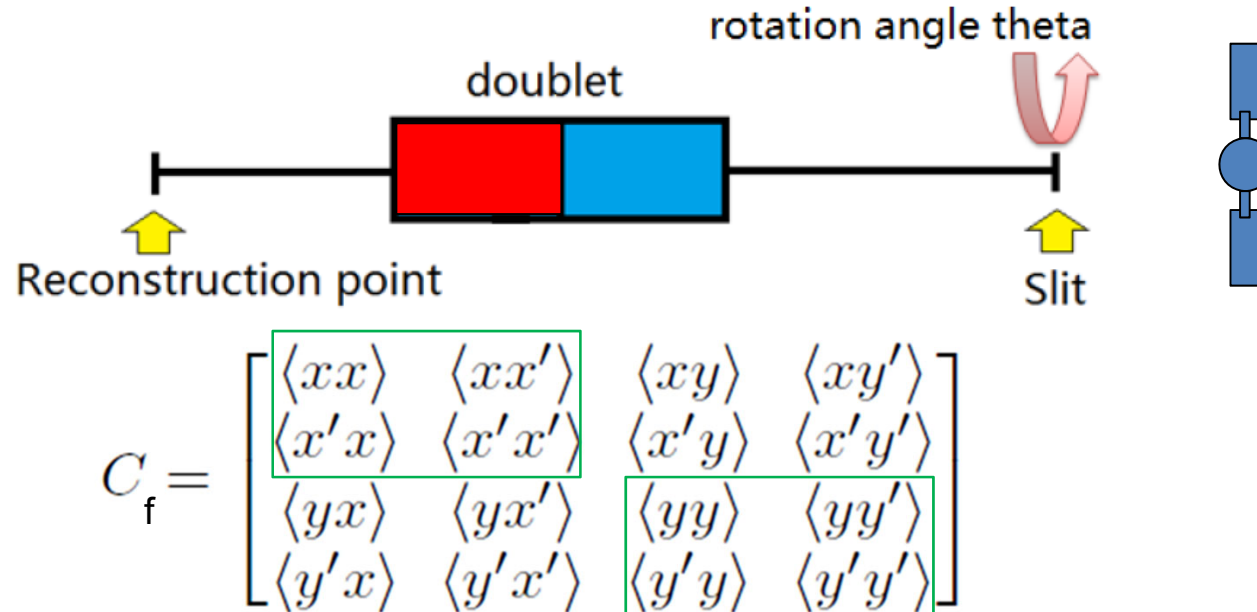
ROSE – measurement principle



All values are measured using Rose behind a magnetic doublet at the final position C_{final} . Knowing the transfer matrix they can be calculated back to the reconstruction point of the original not changing beam matrix C_{initial} . 100% transmission between initial and final Position and full slit-grid coverage is of course required for all magnet settings.

1. $\theta=0^\circ$ magnet setting **a** delivers $\langle xx \rangle_f^a$, $\langle xx' \rangle_f^a$, $\langle x'x' \rangle_f^a$

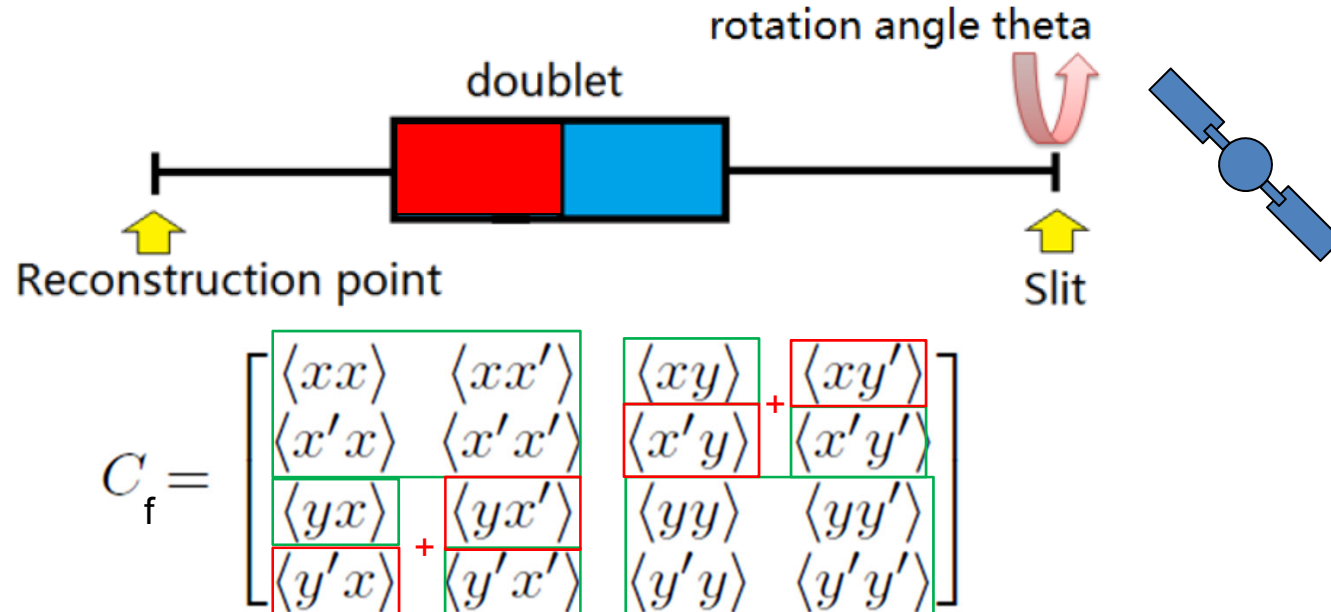
ROSE – measurement principle



All values are measured using Rose behind a magnetic doublet at the final position C_{final} . Knowing the transfer matrix they can be calculated back to the reconstruction point of the original not changing beam matrix C_{initial} . 100% transmission between initial and final Position and full slit-grid coverage is of course required for all magnet settings.

1. $\theta=0^\circ$ magnet setting a delivers $\langle xx \rangle_f^a$, $\langle xx' \rangle_f^a$, $\langle x'x \rangle_f^a$
2. $\theta=90^\circ$ magnet setting a delivers $\langle yy \rangle_f^a$, $\langle yy' \rangle_f^a$, $\langle y'y \rangle_f^a$

ROSE – measurement principle

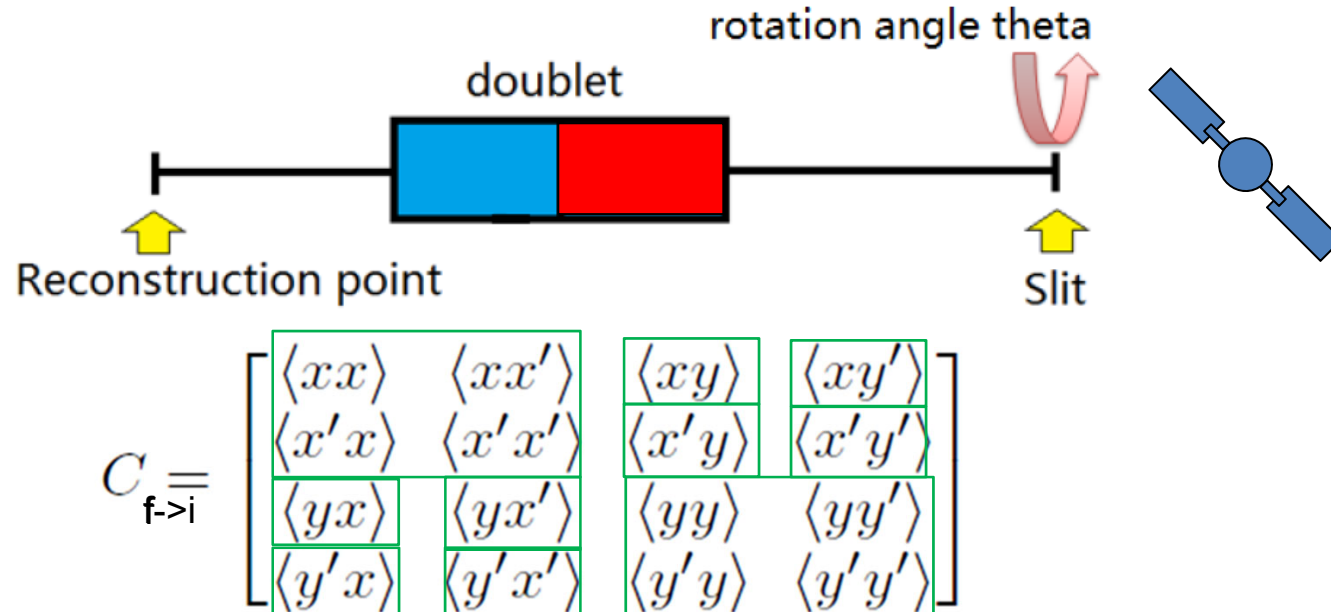


All values are measured using Rose behind a magnetic doublet at the final position C_{final} . Knowing the transfer matrix they can be calculated back to the reconstruction point of the original not changing beam matrix C_{initial} . 100% transmission between initial and final Position and full slit-grid coverage is of course required for all magnet settings.

1. $\theta=0^\circ$ magnet setting a delivers $\langle xx \rangle_f^a$, $\langle xx' \rangle_f^a$, $\langle x'x \rangle_f^a$
2. $\theta=90^\circ$ magnet setting a delivers $\langle yy \rangle_f^a$, $\langle yy' \rangle_f^a$, $\langle y'y \rangle_f^a$
3. $\theta=45^\circ$ magnet setting a delivers $\langle yy \rangle_{\theta}^a$, $\langle yy' \rangle_{\theta}^a$, $\langle y'y \rangle_{\theta}^a$

- Deutsche Patentanmeldung Nr. 102015118017.0
- Rotating system for four-dimensional transverse rms-emittance measurements, C. Xiao, M. Maier, X. N. Du, P. Gerhard, L. Groening, S. Mickat, and H. Vormann, Phys. Rev. Accel. Beams 19, 072802 (2016)

ROSE – measurement principle



All values are measured using Rose behind a magnetic doublet at the final position C_{final} . Knowing the transfer matrix they can be calculated back to the reconstruction point of the original not changing beam matrix $C_{initial}$. 100% transmission between initial and final Position and full slit-grid coverage is of course required for all magnet settings.

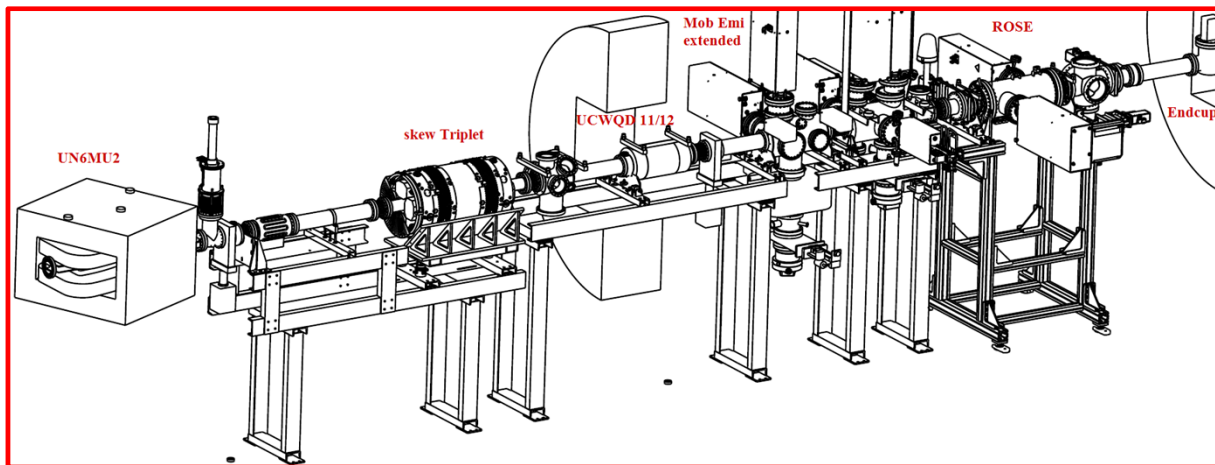
1. $\theta=0^\circ$ magnet setting a delivers $\langle xx \rangle_f^a, \langle xx' \rangle_f^a, \langle x'x \rangle_f^a$
2. $\theta=90^\circ$ magnet setting a delivers $\langle yy \rangle_f^a, \langle yy' \rangle_f^a, \langle y'y \rangle_f^a$
3. $\theta=45^\circ$ magnet setting a delivers $\langle yy \rangle_\theta^a, \langle yy' \rangle_\theta^a, \langle y'y \rangle_\theta^a$
4. $\theta=45^\circ$ magnet setting b delivers $\langle xx \rangle_\theta^b$

only 4 measurements and quite some matrix gymnastics needed to obtain the full beam matrix

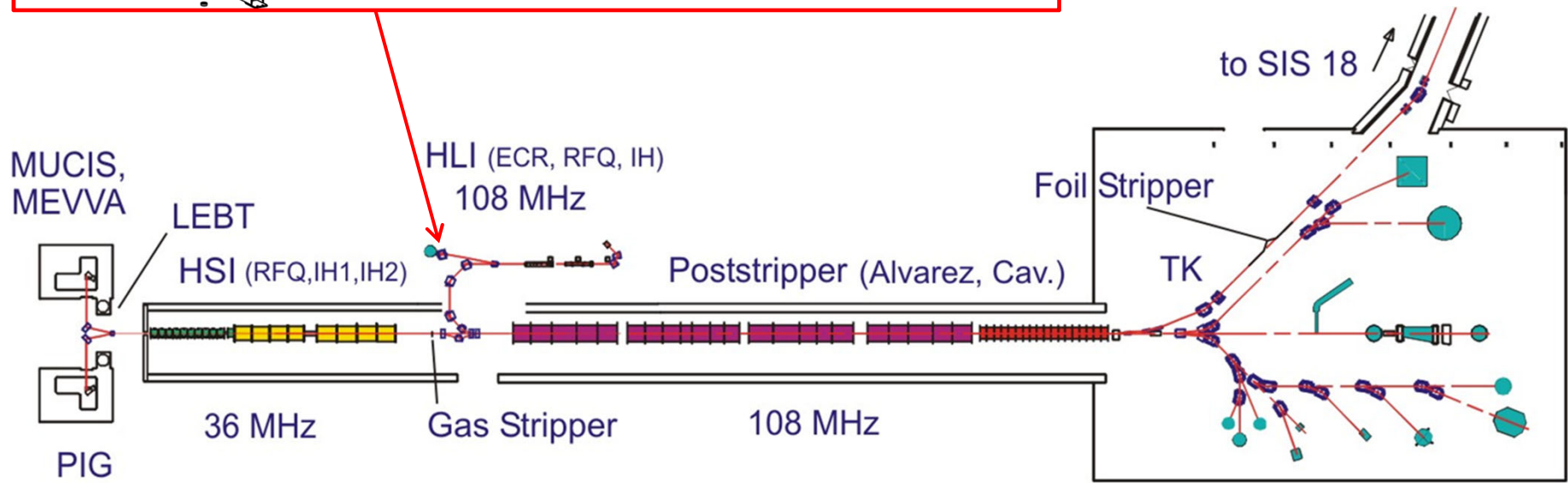
- Deutsche Patentanmeldung Nr. 102015118017.0

- Rotating system for four-dimensional transverse rms-emittance measurements, C. Xiao, M. Maier, X. N. Du, P. Gerhard, L. Groening, S. Mickat, and H. Vormann, Phys. Rev. Accel. Beams 19, 072802 (2016)

ROSE – commissioning setup

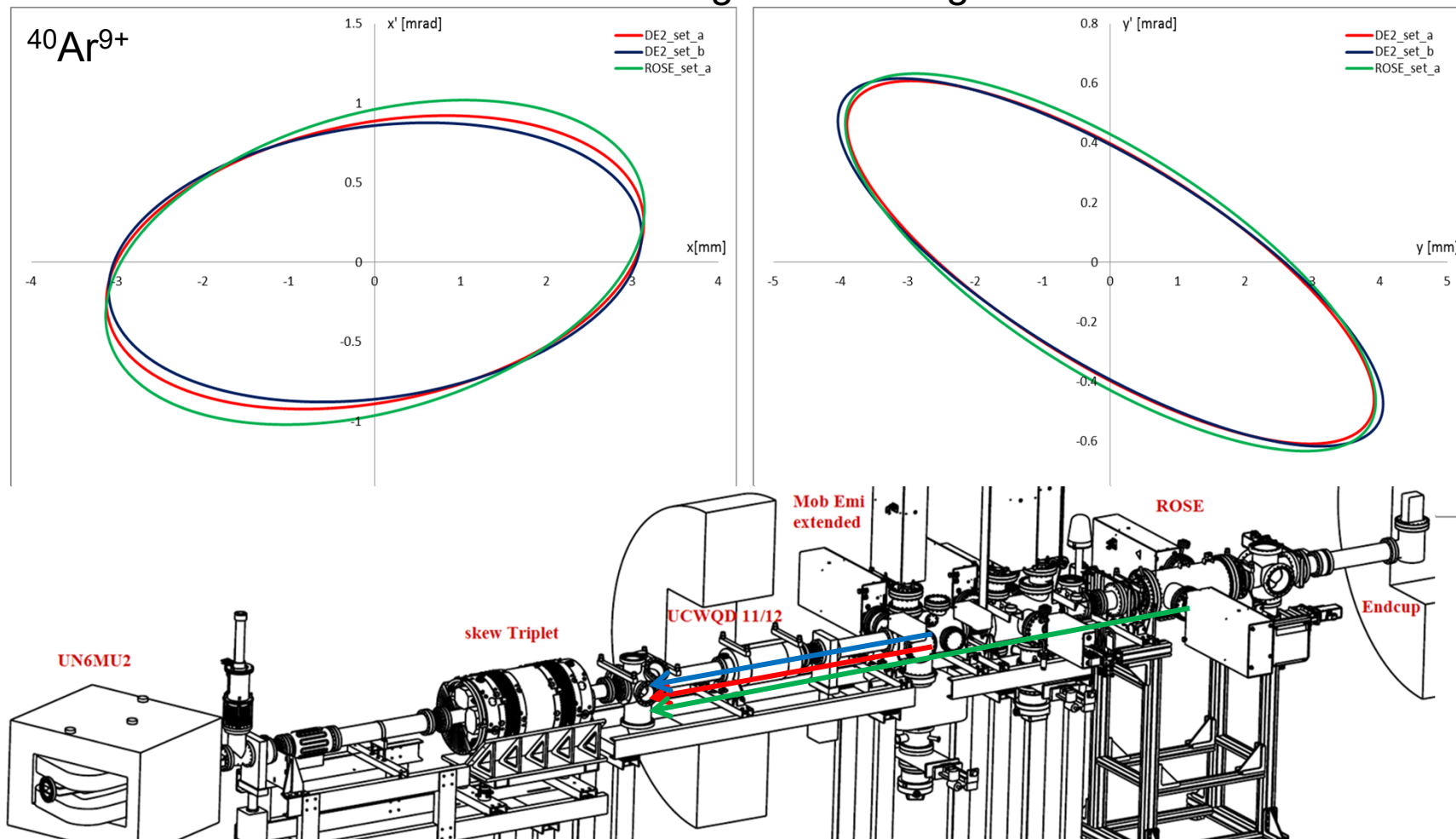


- measurements at exit of GSI's HLI
- 1.4 MeV/u of $^{40}\text{Ar}^{9+}$ and $^{83}\text{Kr}^{13+}$
- skew triplet to create $x \leftrightarrow y$ correlations
- full transmission



ROSE - benchmarking

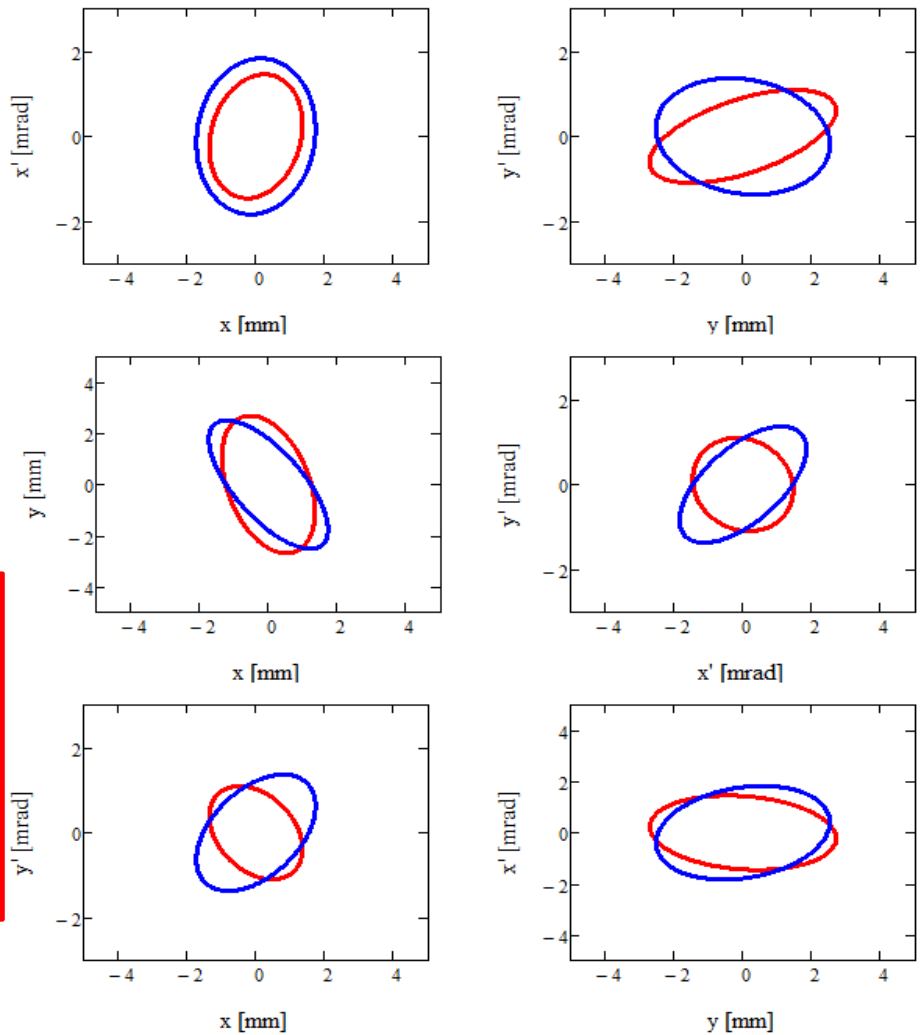
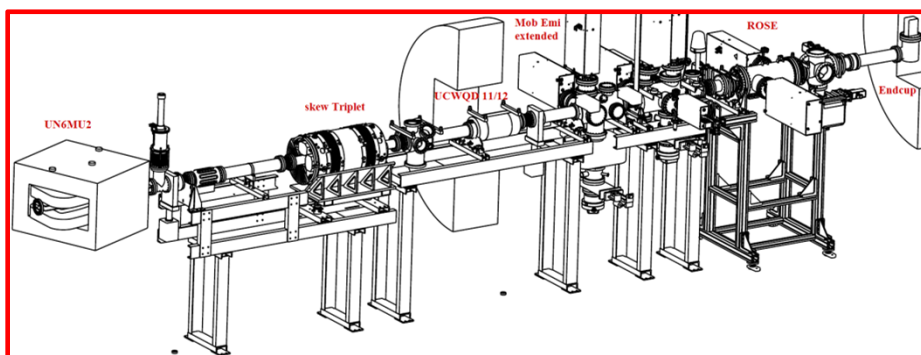
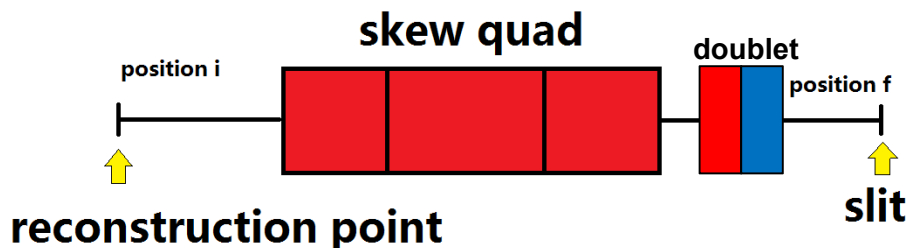
The first commissioning beam time mainly served to commission the hard- and software of ROSE and to benchmark it against existing emittance scanners.



ROSE – proof of principle



measured emittance at the slit



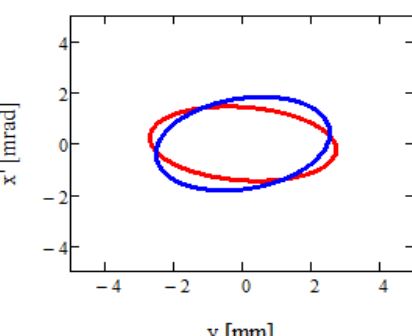
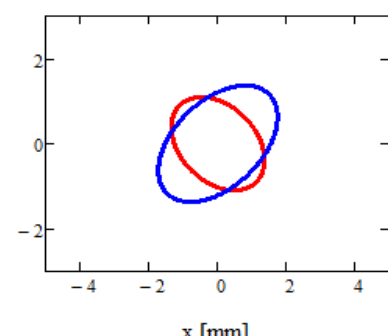
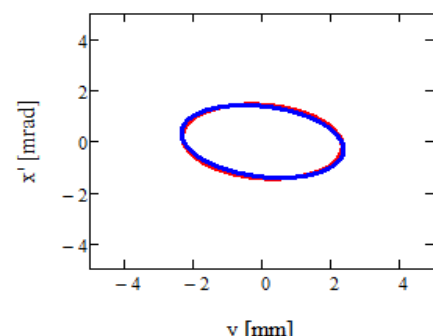
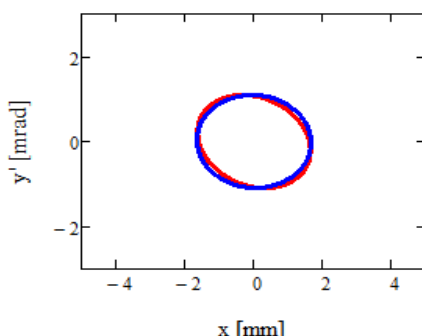
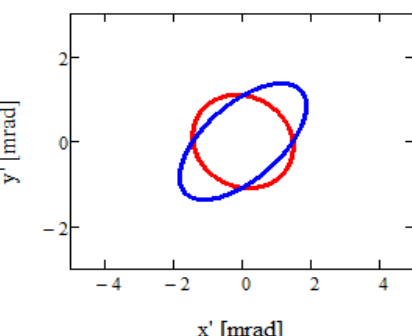
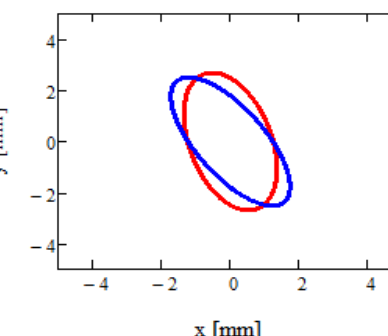
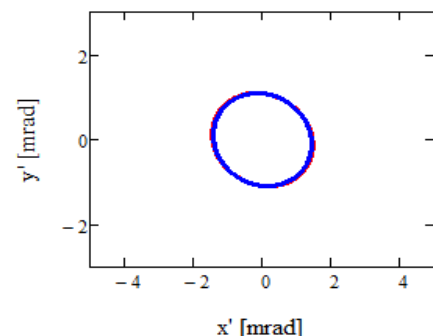
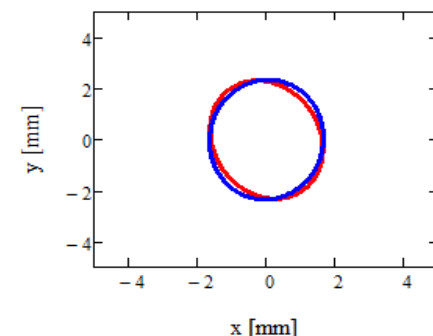
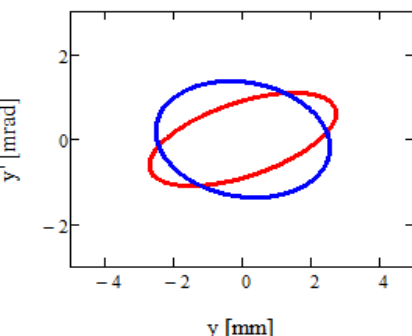
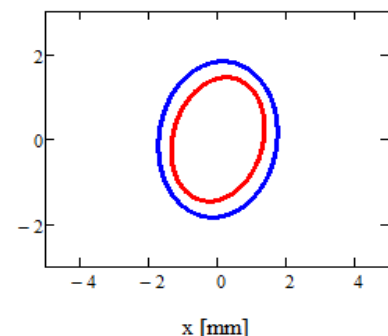
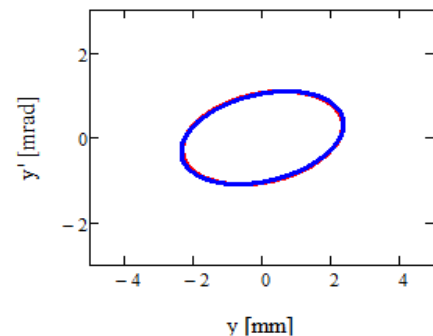
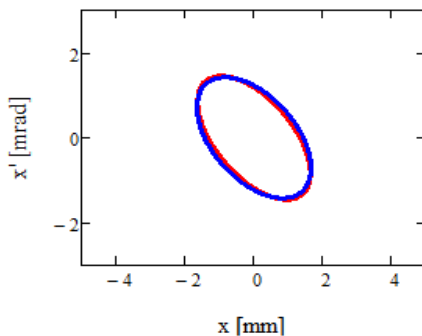
red skew off, blue skew on

ROSE – proof of principle



reconstruction point in front of skew

measured emittance at the slit



red skew off, blue skew on

$\langle RR \rangle$, $\langle PR' \rangle$, and $\langle P'R' \rangle$ at 0° for setting "a".

--- --- --- --- --- 90° --- ---

--- --- --- --- 45° --- ---

45° for setting "b"

beam matrix is a function of

$$M_{\text{beam}} = f \left(\begin{array}{l} \langle PR \rangle^a_{0^\circ}, \langle PR' \rangle^a_{0^\circ}, \langle P'R' \rangle^a_{0^\circ} \\ \langle PR \rangle^a_{90^\circ}, \langle PR' \rangle^a_{90^\circ}, \langle P'R' \rangle^a_{90^\circ} \\ \langle PR \rangle^a_{45^\circ}, \langle PR' \rangle^a_{45^\circ}, \langle P'R' \rangle^a_{45^\circ} \\ \langle PR \rangle^b_{45^\circ}, \langle PR' \rangle^b_{45^\circ}, \langle P'R' \rangle^b_{45^\circ} \end{array} \right)$$

error analysis.

$$\langle RR \rangle^a_{0^\circ} \rightarrow [\langle RR \rangle + \delta_1 \langle RR' \rangle]_{0^\circ}^a = \langle rr \rangle^a_{0^\circ} \quad \left| \frac{\delta \langle RR \rangle}{\langle RR \rangle} \right| \leq 1\% \quad \text{distribution like Gaussian}$$

$$\langle PR' \rangle^a_{0^\circ} \rightarrow [\langle PR' \rangle + \delta_2 \langle PR' \rangle]_{0^\circ}^a = \langle r'n' \rangle^a_{0^\circ}$$

$$\langle P'R' \rangle^b_{45^\circ} \rightarrow [\langle P'R' \rangle + \delta_{12} \langle RR' \rangle]_{45^\circ}^b = \langle r'n' \rangle^b_{45^\circ}$$

$$M_{\text{beam}}(\text{with error}) = f \left(\begin{array}{l} \langle rr \rangle^a_{0^\circ}, \langle r'n' \rangle^a_{0^\circ}, \langle r'n' \rangle^a_{0^\circ} \\ \dots \\ \dots \end{array} \right)$$

↓

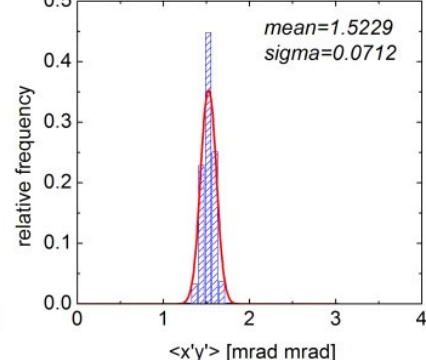
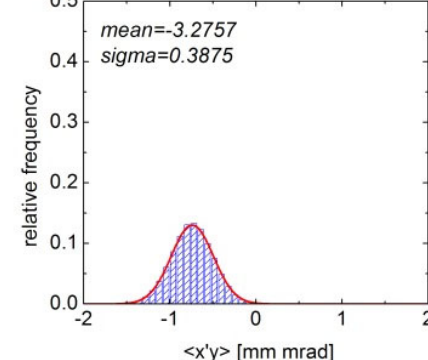
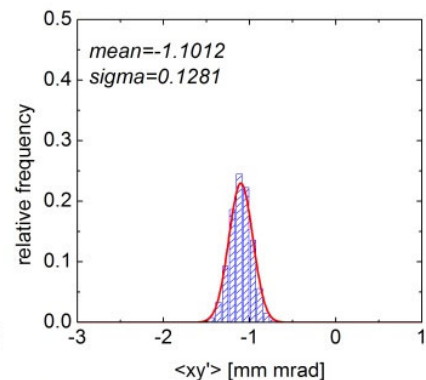
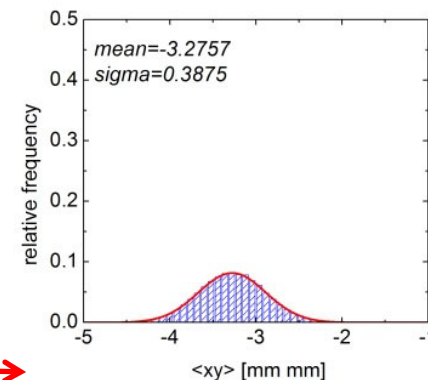
Z_1

Z_2

t



ROSE error studies



Each measured moment entering into the evaluation was varied randomly following a Gaussian distribution centered on its measured value

$\langle RR \rangle$, $\langle PR' \rangle$, and $\langle P'R' \rangle$ at 0° for setting "a".

90°

45°

45° for setting "b"

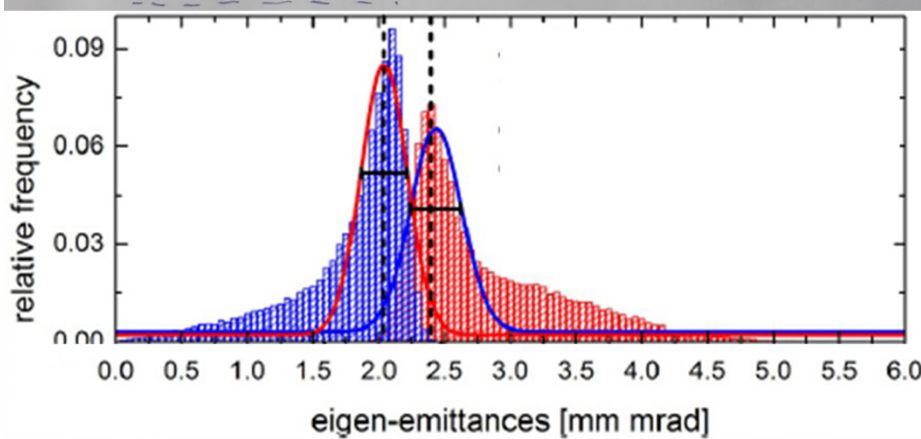
beam matrix is a function of

$$M_{\text{beam}} = f \begin{pmatrix} \langle PR \rangle^a_{0^\circ}, \langle PR' \rangle^a_{0^\circ}, \langle P'R' \rangle^a_{0^\circ} \\ \langle PR \rangle^a_{90^\circ}, \langle PR' \rangle^a_{90^\circ}, \langle P'R' \rangle^a_{90^\circ} \\ \langle PR \rangle^a_{45^\circ}, \langle PR' \rangle^a_{45^\circ}, \langle P'R' \rangle^a_{45^\circ} \\ \langle PR \rangle^b_{45^\circ}, \langle PR' \rangle^b_{45^\circ}, \langle P'R' \rangle^b_{45^\circ} \end{pmatrix}$$

error analysis.

$$\langle RR \rangle^a_{0^\circ} \rightarrow [\langle RR \rangle + \delta_1 \langle RR \rangle]_{0^\circ} = \langle RR \rangle^a_{0^\circ} \quad \left| \frac{\delta \langle RR \rangle}{\langle RR \rangle} \right| \leq 1\% \quad \text{distribution like Gaussian}$$

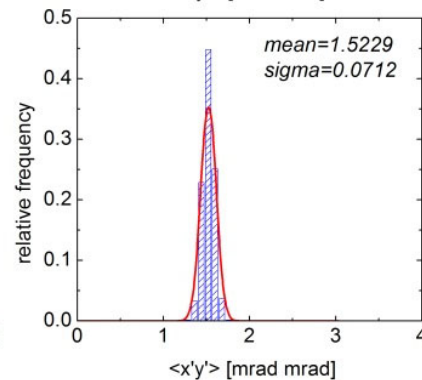
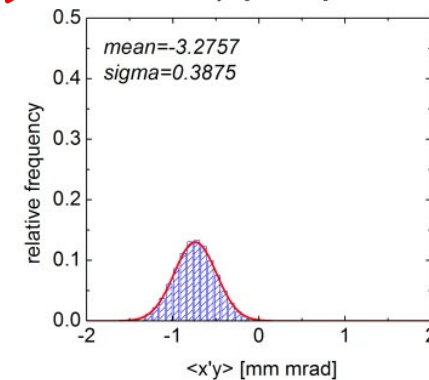
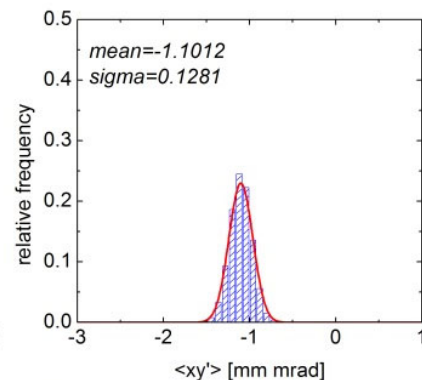
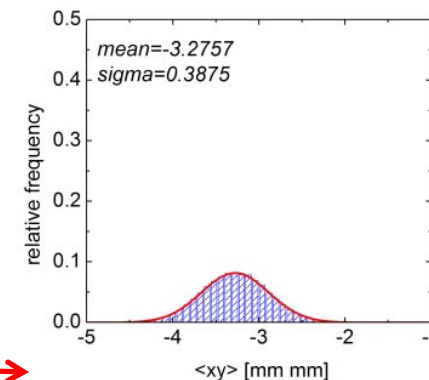
$$\langle PR' \rangle^a_{0^\circ} \rightarrow [\langle PR' \rangle + \delta_2 \langle PR' \rangle]_{0^\circ} = \langle PR' \rangle^a_{0^\circ}$$



From the measured moments derived Eigen-emittances of the HLI 1.4 MeV/u $^{83}\text{Kr}^{13+}$ beam.



ROSE error studies



Each measured moment entering into the evaluation was varied randomly following a Gaussian distribution centered on its measured value

ROSE – intermediate summary

- We have measured the 4d beam parameters of a $^{238}\text{U}^{28+}$ beam with a kinetic energy of 11.4 MeV/u using the skew technique.
- We have developed and successfully commissioned ROSE, a prototype 4d emittance scanner that is independent of ion-species, -current and -energy.
- In the future we would like to
 - decouple the $^{238}\text{U}^{28+}$ beam using the skew triplet confirming it with ROSE
 - repeat EMTEX creating a flat beam accompanied by ROSE
 - build a two chamber system to gain flexibility and to reduce measurement time
 - And for curiosity we could use the skew to rotate the beam followed by a regular Quadrupole triplet to decouple the beam in its new coordinate system!
- With **NTG Neue Technologien GmbH & Co. KG** we have found an industrial partner. Together we are planning to develop a turnkey 4d emittance scanner for the ion accelerator community.



ROSE – as a customer product



To develop a turnkey 4d emittance scanner three parts have to be considered:

**hardware
electronics
software**

Alle three parts should be as flexible and independent as possible of external resources!

- **The hardware** should cover a maximum range of absolute emittance size while simultaneously guaranteeing the best achievable accuracy.
- **The electronics** should be able to control and perform and save the measurement without the backbone of an accelerator control system using a beam trigger in case of pulsed beams, delivering and accepting the necessary signals to trigger interlocks.
- **The software** should guide the user through planning, performing and evaluating the different measurements.

NTG – Neue Technologien GmbH & Co. KG, Gelnhausen, Germany

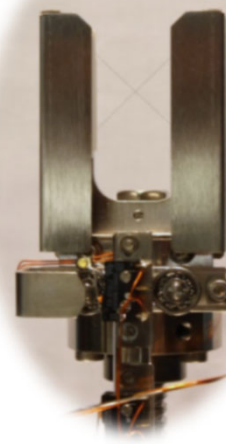
Faraday Cups Slow and 50Ω



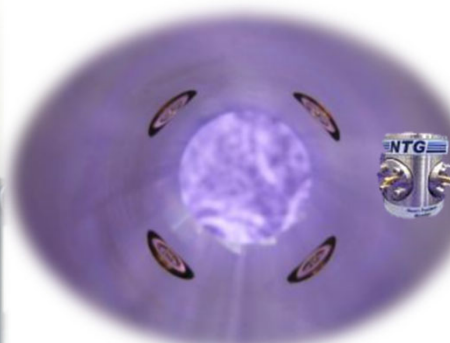
profile grids



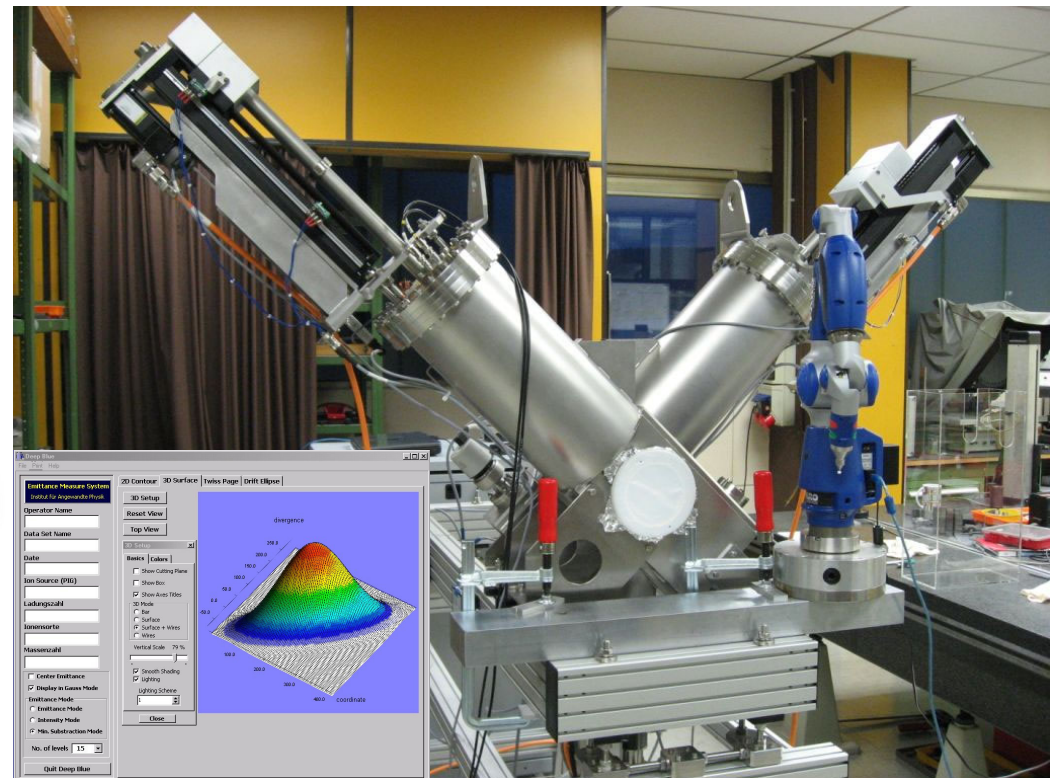
wire Scanners



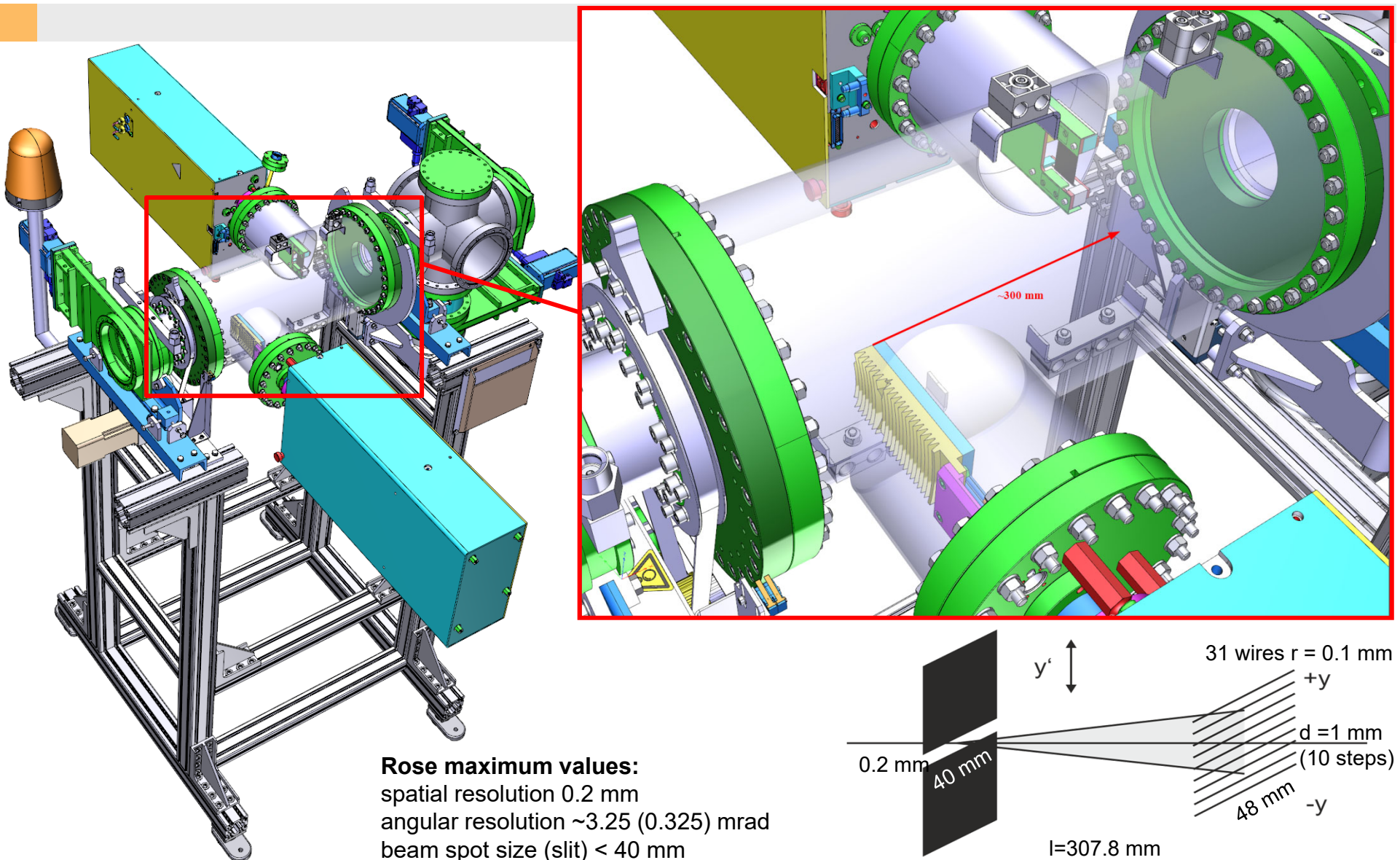
capacitive BPMs



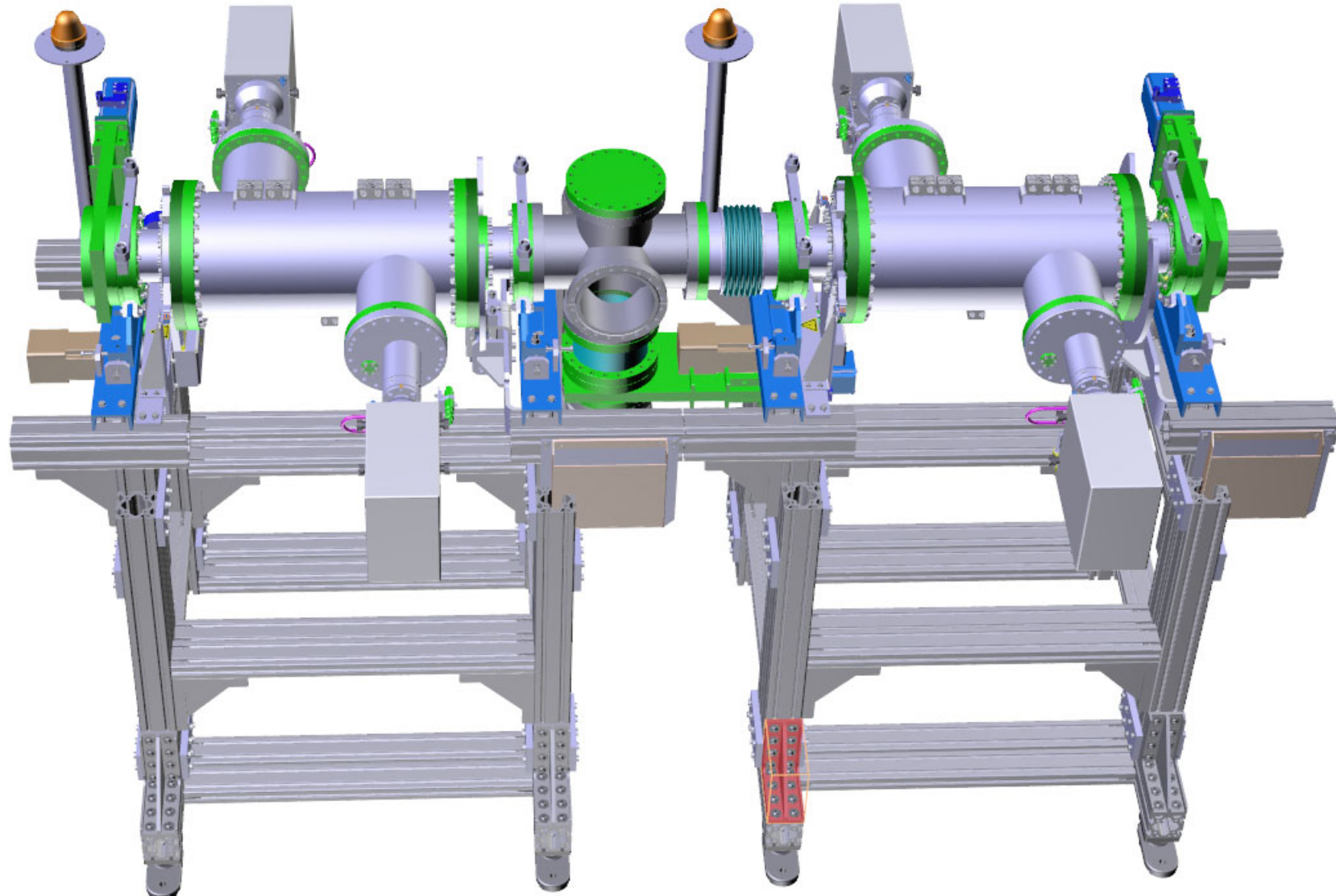
Emittance measuring system based on a stepping motor driven crossed slit and a profile grid.



ROSE – Hardware existing



ROSE – Hardware modified for flexibility



ROSE – stand alone electronics

ROBOMAT* a modern version of our old:

Pelomat from the mid 90's using grid electronics of the 80's



The technical details and requirements have been discussed with NTG our beam diagnostics- and the Linac-department and on this base NTG has made an offer.

The key features are:

- rotation of ROSE
- performing emittance measurements
- capability to measure DC and pulsed beam 250kHz
- total beam currents ranging 10µA - 100mA
- ion current measurement for normalization
- diverse in/out going interlock signals:
 - (in) beam on / trigger / gate
 - (out) moving device
 - (out) vacuum pressure
 - (out) slit water cooling
 - (out) gate valve status
 - ...
- emittance data format XML

*

Gefördert durch:



Bundesministerium
für Wirtschaft
und Energie

aufgrund eines Beschlusses
des Deutschen Bundestages

The ROBOMAT electronics



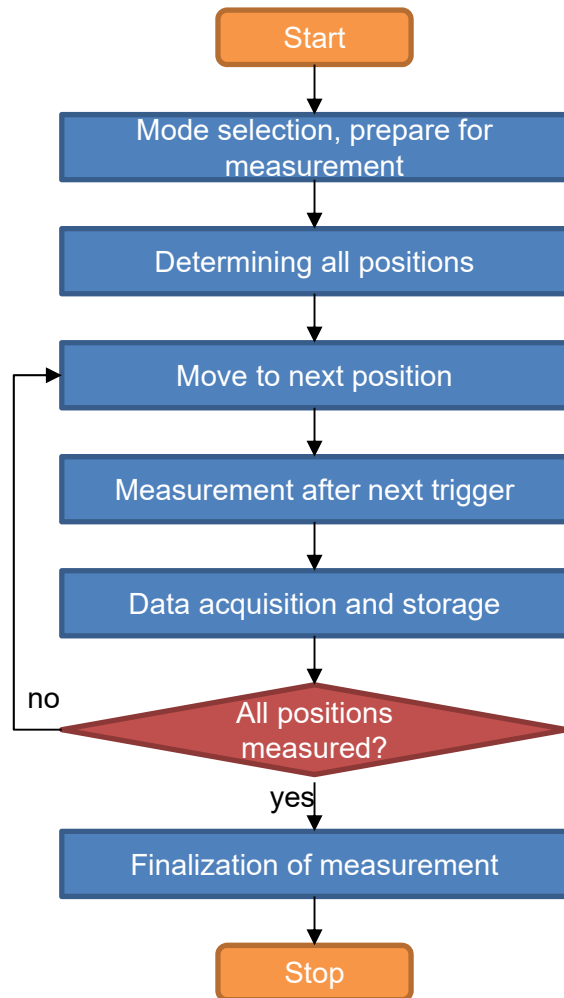
Thirty-two parallel multi-range current to voltage converter channels

- Bipolar inputs, bandwidth DC to 250 kHz
- Dynamic range <1 nA to 10 mA over four measurement ranges
- Thirty-two 14 bit 1 MHz ADCs for fully parallel sampling; digital down-sampling to increase effective resolution



The grid electronics Pyramid F3200E that will be used for the ROBOMAT has arrived at NTG and is currently prepared, tested and commissioned. Also the stepper motor and associated controller units have arrived at NTG and will be integrated into our prototype ROSE to replace our GSI systems

ROBOMAT key features

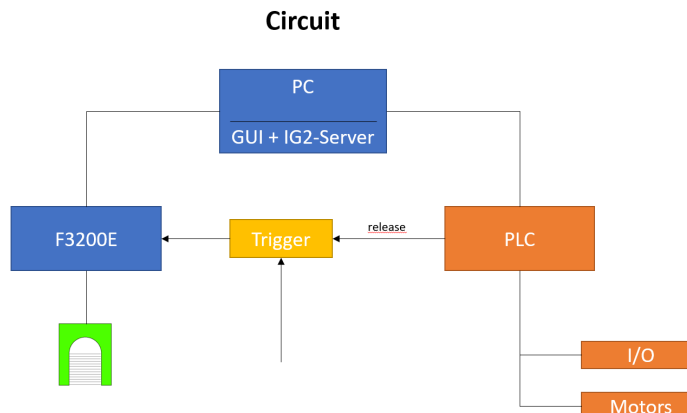


Measurement Modes:

- parallel: - slit and grid are moving in parallel.
- ang. offset: - slit and grid move together with an offset for the grid.
- double grid: - for each slit position there are two grid positions (double angle range).
- diagonal: - slot is moved with offset, which is a function grid position.
- ultrafast: - measurement while moving.
- profile grid: - only the grid is driven into the beam.
- background: - measurement without beam.

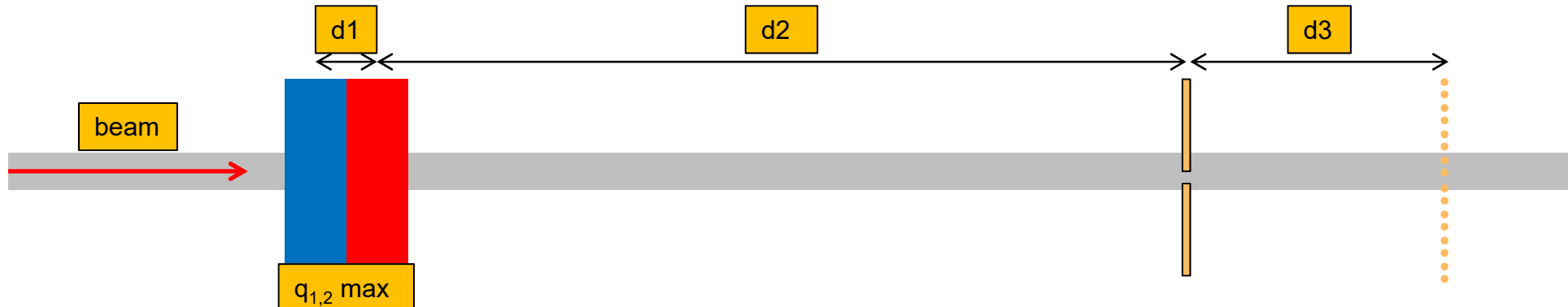
By means of the selected modes, the positions for slot and grid are determined, which are to be approached. This can be graphically displayed, if necessary. Subsequently, the settings are transmitted to the electronics and the measurement is performed.

With the "Ultrafast" option, the beam signals are stored during a constant speed movement. This procedure is triggered by the accelerator. After completing the measurement, the data is transferred to the PC and displayed. Thus, a rough picture of the emittance can be obtained for verification of the validity of the measurement settings.



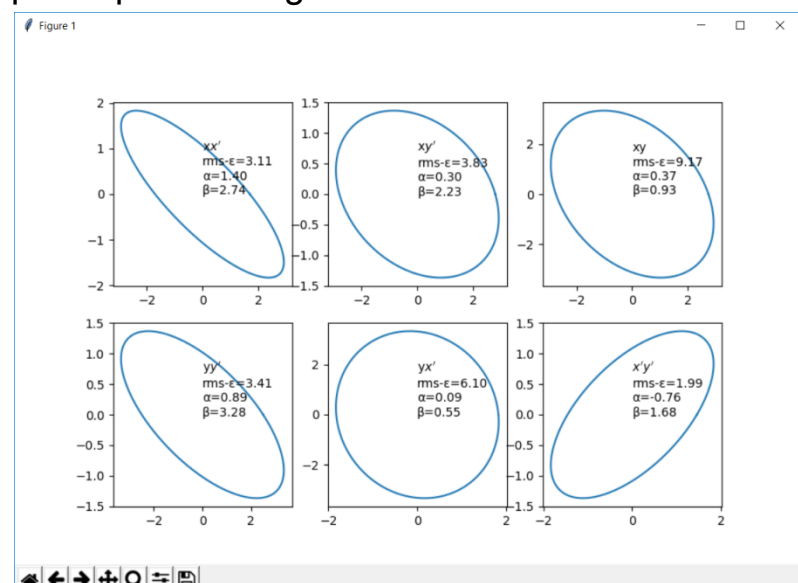
ROSE – software package

Guiding the user through ROSE 4d emittance measurements

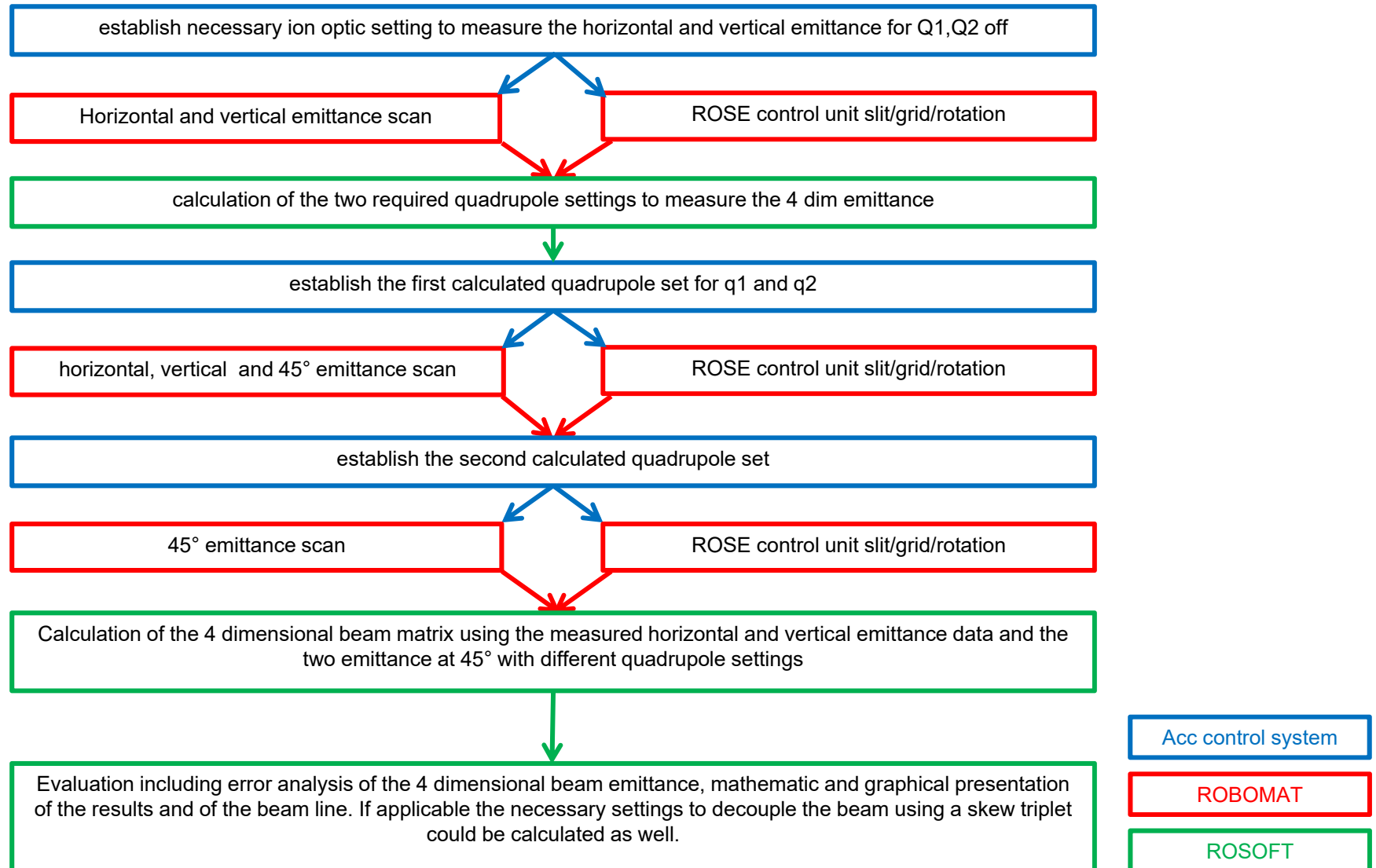


1. User entry of basic information e.g. beam line geometry and maximum field strength, beam parameters
2. User selection of measurement mode: profile grid, 2d-, **4d-emittance**
3. 2d emittance with quadrupoles off to determine optimum quadrupole settings for the 4d-emittance
4. 4d emittance using the above quadrupole settings
5. Numerical and graphical evaluation of the 4d-Emittance

C:
8.5400 -4.3485 -3.4124 -1.1521
-4.3485 3.3496 -0.5442 1.5196
-3.4124 -0.5440 11.2004 -3.0488
-1.1520 1.5197 -3.0488 1.8700
eigen ϵ_1 : 2.4451 eigen ϵ_2 : 1.9345



ROSE – software package



Thank you very much for your attention

My special gratitude goes to all co-workers and funding agencies:

GSI staff of:

- LINAC department
- TTR technology transfer
- BEA beam instrumentation
- MDS mechanical design
- MEW mechanical workshop
- TRI transport and installation
- VAC accelerator vacuum

The staff of the company



And last but not least
the funding agencies:

Gefördert durch:



aufgrund eines Beschlusses
des Deutschen Bundestages